agriculture

MDPI

Article

Applying Silver Nanoparticles to Enhance Metabolite Accumulation and Biodiesel Production in New Algal Resources

Maria Hasnain [1], Neelma Munir [1], Zainul Abideen [2,*], Daniel Anthony Dias [3], Farheen Aslam [1] and Roberto Mancinelli [4,*]

1 Department of Biotechnology, Lahore College for Women University, Lahore 35200, Pakistan
2 Dr. Muhammad Ajmal Khan Institute of Sustainable Halophyte Utilization, University of Karachi, Karachi 75270, Pakistan
3 School of Health and Biomedical Sciences, Discipline of Laboratory Medicine, RMIT University, P.O. Box 71, Bundoora, VIC 3083, Australia
4 Department of Agricultural and Forest Sciences (DAFNE), University of Tuscia, 01100 Viterbo, Italy
* Correspondence: zuabideen@uok.edu.pk (Z.A.); mancinel@unitus.it (R.M.)

Abstract: Biofuel generation from algae can be increased by using nanotechnology. The present study emphasizes the use of silver nanoparticles on algae for algal fuel generation along with the impact of nanoparticles on biomass, metabolites and lipid profile. Silver ion amassing was enhanced in each algal species, but maximum phytoremediation was found in *Ulothrix* sp. Carbohydrates increased 3.2 times in *Oedogonium* sp., 3.3 times in *Ulothrix* sp., 3 times in *Cladophora* sp. and 2.7 times in *Spirogyra* sp. Additionally, the application of nanoparticles enhanced by 2 times the production of proteins in *Oedogonium* sp., 1.9 times in *Ulothrix* sp., 1.9 times in *Cladophora* sp. and 2.1 times in *Spirogyra* sp. Finally, the total lipid yield increased 60% DCW in *Oedogonium* sp., 56% DCW in *Ulothrix* sp., 58% DCW in *Cladophora* sp. and 63% DCW in *Spirogyra* sp. using 0.08 mg/L silver nanoparticle application. The lipids and fatty acid fractions from algae containing high concentrations of C16:0, C18:0 and C18:1 enhanced with silver nanoparticle addition were comparable with EN 14214 and ASTM 6751 biodiesel standards. This study indicates that the uptake of AgNPs can enhance the production of fatty acids and be commercialized as sustainable biodiesel. The algae *Ulothrix* sp. is evidenced as the best competent feedstock for biofuel production.

Keywords: silver nanoparticles; carbohydrates; proteins; lipids; algae biomass; biodiesel; fuel properties

check for updates

Citation: Hasnain, M.; Munir, N.; Abideen, Z.; Dias, D.A.; Aslam, F.; Mancinelli, R. Applying Silver Nanoparticles to Enhance Metabolite Accumulation and Biodiesel Production in New Algal Resources. *Agriculture* **2023**, *13*, 73. https://doi.org/10.3390/agriculture13010073

Academic Editor: Jin Liu

Received: 12 November 2022
Revised: 12 December 2022
Accepted: 20 December 2022
Published: 26 December 2022

1. Introduction

Increasing population, industrialization and fossil fuels depletion have triggered an energy crunch and, thereby, global warming. On the other hand, demands for fuel have also risen due to climatic changes and unstable fossil fuel production worldwide. The production of energy from edible crops to fulfill energy requirements has negatively affected the agro-ecological system [1]. On the other hand, the biofuels generated from algae are less hazardous to the environment because of their lessened dependency on land and freshwater resources. Due to their high growth rate, algae possess high productivity in short harvesting cycles, usually 1–10 days, as compared to other feedstocks (two times a year) [2]. Moreover, they have the capacity to sequester carbon 10 to 50 times higher than other land plants. Algal fuels have not touched commercial production yet due to limitations in biomass harvesting. Approaches to improve the biomass of algae and efficient production of fuel suggest the application of nanoparticles. Nanoparticles can stimulate the primary metabolite production and enrich lipid sources to enhance biofuel production. To enhance the fatty acid conversion efficacy to biodiesel fuel, the use of nanoparticles is recommended

for proper lipid extraction or cell division [3]. The application of nanoparticles in the cultivation medium increases growth, carbon dioxide absorption from the air and light conversion efficiency. Therefore, the addition of nano-additives is a contemporary effective method to improve biomass yield, carbohydrates and lipids with regard to bioethanol, biomethane and biodiesel. However, the addition of nanoparticles to algal cultures is not an easy method, and numerous aspects must be considered concerning the concentration and characteristics of the nanoparticles [4].

Silver nanoparticles (AgNPs) have broad applications in food (especially in food packaging), cosmetics (in moisturizer, makeup and hair care products) [5], clothing and in the environmental sector (water and air purification) [6]. Global nanomaterial application has already contaminated the ecosystem, mainly silver nanomaterial. Nano-silver has badly affected water organisms; the production of these particles was 320 to 420 tons/year in 2016 (still increasing) and expected to reach 800 tons by 2025, which is of serious concern [7]. To maintain and improve a sustainable and "green" environment, renewable and environmentally friendly energy feedstocks are required to reclaim current environmental issues. In an aquatic ecosystem, phytoplankton (algae) can undergo physiological modification and accumulate AgNPs [8].

Algae are a significant producer of energy and food cradle, contributing 40% of global biomass productivity and assisting in water purification. NPs cause membrane and mitochondrial damage, lysis, mutations and growth retardation. However, algae have a setup of responses (biochemical and molecular) against contaminants allowing them to adapt and protect themselves, such as the antioxidative defense system to exclude ROS and secretion of biomolecules to form a protective layer [9]. *Oedogonium* sp., Ulothrix sp., *Cladophora* sp. and *Spirogyra* sp. hold great capability to remediate waste resources and emerging pollutants. Nevertheless, these practical approaches to facilitate microalgal applications in a commercially feasible manner need to be improved, as performed in this experiment [2].

The impact of silver nanoparticles on green algae has been well-documented in many recent studies. For example, AgNPs perturbed the cell wall of algae and stimulated the discharge of intracellular metabolites suitable to produce biofuel. Silver nanoparticle–algae interactions trigger the reactive oxygen species (ROS) that modify metabolic pathways for the fabrication of hydrocarbons. The following hypotheses were assessed in this investigation: (1) absorbance of AgNPs by algae is helpful in bioremediation of polluted soil, (2) the exposure of AgNPs will increase photosynthesis pigment and algal biomass and (3) AgNPs will enhance the production of carbohydrates, proteins and lipids for biofuel production. This study was planned to improved biodiesel quantity with quality via nanotechnology from algae. The present study anticipates that the nanoparticle application can trigger the storage of algal metabolites with bioremediation via algal resources.

2. Material and Methodology

2.1. Sampling and Identification of Algae

Different species of algae were collected from different areas of Punjab, Pakistan. Four algal strains were selected on the bases of morphology and further recognized by matching 18SrDNA and ITS regions. After DNA extraction [10], the 18SrDNA gene was amplified and sequenced using Macrogen, then sequences were used to draw phylogenetic trees using MEGAX software.

2.2. Response Surface Methodology (RSM) Design

RSM (DESIGN-EXPERT 11) was used to elevate the conditions of silver nanoparticles for the optimal production of carbohydrates, proteins and lipids for algal biomass production. The experimental design consisted of AgNPs (Sigma® St. Louis, MI, USA) ranging from 0 to 0.08 mg/L and days 1 to 7 as design variables and growth, carbohydrates, proteins, chlorophyll and lipids as response variables. Tables 1 and 2 depict the optimized variables for all the tested algal strains, with 13 trials in total. Firstly, 5 g FW of each alga was inocu-

lated in 500 mL jars with Blue Green (BG) media (Table S1 in Supplementary Data) at pH 7, 25 °C, under a 16 h:8 h light–dark cycle. On days 1, 3, 5, 7 and 8, biomass was harvested.

2.3. Quantification of Silver Uptake Using Atomic Absorption Spectrophotometry

To determine the concentration of silver present in the four algae, Z-5000 polarized Zeeman atomic absorption spectrophotometry was used according to the protocol mentioned in [11].

2.4. Algal Growth

Algae biomass was calculated after the implication of nanoparticles. Biomass productivity was calculated by using this formula:

$$\text{Biomass productivity (g FW)} = \text{Amount of biomass (g)/Number of days} \quad (1)$$

2.5. Biochemical Profiling

Carbohydrates, total protein, chlorophyll and lipids were quantified. Dry algae (10 mg) were used for quantification of carbohydrates by following the protocol mention in [12], while 1 mg dry algae were used to quantify total protein followed by that in [2]. Chlorophyll estimation using methanol was performed on 0.5 g of algae [13]. One gram of dried algal sample was used to extract lipids via microwave-assisted extraction. Lipid contents were calculated in percentage by using the following formula [14].

$$\text{Lipid content (\% DCW)} = (\text{weight of lipids/weight of samples}) \times 100 \quad (2)$$

2.6. Transesterification and FAME Analysis via GC-MS

Extracted lipids were transesterified using 1.5 (wt.%) KoH as a catalyst with 1:6 lipids: methanol ratio at 60 °C for 120 min; the top layer was isolated from the glycerol then centrifuged for 10 min at 13,000× *g*. The biodiesel was washed with deionized water [14]. After transesterification, the recovered FAMEs were injected into a GC-MS (Agilent Technologies 7890B, Santa Clara, CA, USA) with the GCMS condition mentioned in [15].

2.7. Fuel Properties Determined from the Fatty Acid Profile Generated from GCMS

Fuel properties, including higher heating value, cetane number, iodine value, saponification valve, oxidation stability, cold filter plugging point, density, and kinematic viscosity, were calculated using the formulas mentioned in [16].

2.8. Statistical Analyses

Analysis of variance (ANOVA) and a least significant difference was performed to analyze the data of central composite design (DESIGN-EXPERT 11).

3. Results and Discussion

3.1. Molecular Identification of Algae

Algae used during present study were molecularly characterized via PCR. The phylogenetic tree indicated that KU865576 had 94% similarity with *Oedogonium* sp. (Figure S1 in Supplementary Data). The second sample LHRZOO6 with an accession number of KU865575 s showed the closest similarity of (92%) with *Ulothrix zonata* (JX491152.1). JGDN5, assigned with accession no. KU865580, showed closest similarity (84%) with *Cladophora* sp. (KF318887.1). PUL1 (KU865578) showed 93% homology with *Spirogyra* sp. (KM677012.1).

3.2. Bioremediation of Silver Nanoparticles by Algal Species

The capacity of the four algal strains to remediate silver ions with respect to days is shown in Table 1. *Ulothrix* sp. attained the maximum uptake of silver ions sp. at 0.00149 mg/g (9.3% removal), with 0.00144 mg/g (9%) by *Cladophora* sp., 0.00142 mg/g

(8.8%) by *Spirogyra* sp. and 0.00137 mg/g (8.5%) by *Oedogonium* sp. The algal cell wall is an essential part in the bioremediation of AgNPs as it provides sites for interaction and acts as a barrier for translocation. Algal blooms depend on the cell wall thickness (5–20 nm) to resist silver deposition, which defines its barrier properties [17]. Although algal cell walls are semi-permeable and permit limited passage of small particles, the AgNP uptake depends on the algal cell size and shape with charge. The application of AgNPs permits the formation of new pores in the algal membrane, making them more permeable and less selective in facilitating transportation [18]. AgNPs can pass across the algal cell membrane via transportation and ion/voltage-gated channels, subsequently reaching the cytosol, binding to cellular organelles and reducing ROS formation, improving photosynthetic and respiratory processes [19]. Application of a low concentration of AgNPs (0.08 mg/L) seems feasible for each studied algae to absorb AgNPs; however, *Ulothrix* sp. absorbed a high quantity of AgNPs compared to other strains. Hence, all of these four strains could be used to amass silver from silver-contaminated water.

Table 1. Central composite design results from silver ion uptake by algae.

		Factor 1	**Factor 2**	**Response 1**	**Response 2**	**Response 3**	**Response 4**
Std	**Run**	**A: Silver Nanoparticle**	**B: Days**	***Oedogonium* sp.**	***Ulothrix* sp.**	***Cladophora* sp.**	***Spirogyra* sp.**
		mg/L		**mg/g**	**mg/g**	**mg/g**	**mg/g**
5	1	0.05	5	0.00105	0.00114	0.00111	0.00109
13	2	0.02	3	0.00053	0.00062	0.00059	0.00057
2	3	0.02	5	0.00072	0.00081	0.00078	0.00076
9	4	0.02	7	0.00094	0.00102	0.00099	0.00097
11	5	0.05	5	0.00103	0.00114	0.00111	0.00109
6	6	0.08	7	0.00137	0.00149	0.00144	0.00142
3	7	0.02	5	0.00072	0.00081	0.00078	0.00076
12	8	0.05	5	0.00105	0.00114	0.00111	0.00109
7	9	0.08	3	0.00093	0.00105	0.00101	0.00099
10	10	0.05	8	0.00122	0.00135	0.00131	0.00129
8	11	0.05	3	0.00074	0.00085	0.00081	0.00078
1	12	0.05	5	0.00105	0.00114	0.00111	0.00109
4	13	0.05	5	0.00105	0.00114	0.00111	0.00109

3.3. Effect of Silver Nanoparticles on Algal Growth

The effect of AgNps reduced the growth of *Oedogonium* sp. from 5 g to 1.8 g, 2.3 g in *Ulothrix* sp., 1.5 g in *Cladophora* sp., and 1.3 g in *Spirogyra* sp. with respect to days under a concentration of 0.08 mg/L on day 7 (Table 2). The production of free radicals in algae damages cellular functions, which reduces the growth of these strains [20]. In one report, a concentration of 1 mg/L titanium NPs reduced *Dunaliella salina* growth [21]. Fe_2O_3 nanoparticles reduced the growth of the alga *Scenedesmus obliquus* on day 7 with a reduction of 8.0, 14.7 and 16.9% at 40, 60 and 100 mg/L, respectively [22]. MgO nanoparticles reduced growth by 22.7, 35.4 and 41.1% under 0.8, 8 and 40 mg/L on day 7, respectively, due to the formation of agglomerates from NPs restricting the penetration of light, severely affecting algal growth [23].

Table 2. The central composite design of combined effect of silver nanoparticles, metabolites and stress duration (Days) in algal strains.

Std	Run	Factor 1	Factor 2	Algal Strain	Response 1	Response 2	Response 3	Response 4	Response 5
		A: Silver Nanoparticle (mg/L)	B: Days		Growth (g FW)	Carbohydrates (mg/g)	Proteins (mg/g)	Chlorophyll (µg/gfw)	Lipids (%)
8	1	0	1	*Oedogonium* sp.	5	0.15	0.019	40	46
				Ulothrix sp.	5	0.14	0.020	34	50
				Cladophora sp.	5	0.17	0.022	38	48
				Spirogyra sp.	5	0.2	0.017	35	44
9	2	0.02	3	*Oedogonium* sp.	5.3	0.16	0.021	39	48
				Ulothrix sp.	6	0.17	0.022	33	51
				Cladophora sp.	6.2	0.20	0.025	37	50
				Spirogyra sp.	5.1	0.24	0.020	35	45
1	3	0.02	5	*Oedogonium* sp.	3.3	0.18	0.023	34	49
				Ulothrix sp.	4.4	0.16	0.024	27	53
				Cladophora sp.	3.6	0.2	0.026	32	51
				Spirogyra sp.	3.3	0.23	0.021	29	47
7	4	0.02	7	*Oedogonium* sp.	2.7	0.21	0.026	29	53
				Ulothrix sp.	3.5	0.19	0.027	23	56
				Cladophora sp.	2.7	0.23	0.028	27	54
				Spirogyra sp.	2.4	0.26	0.024	25	51
4	5	0.05	5	*Oedogonium* sp.	3.0	0.45	0.031	32	67
				Ulothrix sp.	4	0.41	0.032	25	71
				Cladophora sp.	3.2	0.45	0.034	30	69
				Spirogyra sp.	2.9	0.48	0.029	27	65
11	6	0.08	7	*Oedogonium* sp.	1.8	0.49	0.038	19	74
				Ulothrix sp.	2.3	0.47	0.039	13	78
				Cladophora sp.	1.5	0.51	0.042	17	76
				Spirogyra sp.	1.3	0.54	0.036	15	72
12	7	0.02	5	*Oedogonium* sp.	3.3	0.18	0.023	34	52
				Ulothrix sp.	4.2	0.16	0.024	27	56
				Cladophora sp.	3.4	0.2	0.026	32	54
				Spirogyra sp.	3.3	0.23	0.021	29	49
13	8	0.05	5	*Oedogonium* sp.	3	0.43	0.031	32	67
				Ulothrix sp.	4	0.41	0.032	25	71
				Cladophora sp.	3.2	0.45	0.034	30	69
				Spirogyra sp.	2.9	0.48	0.029	27	65
10	9	0.08	3	*Oedogonium* sp.	3.8	0.47	0.036	21	61
				Ulothrix sp.	4.8	0.45	0.037	15	65
				Cladophora sp.	4	0.49	0.039	19	63
				Spirogyra sp.	3.7	0.51	0.034	17	59
6	10	0.05	8	*Oedogonium* sp.	2.2	0.45	0.034	28	68
				Ulothrix sp.	3.2	0.43	0.035	21	72
				Cladophora sp.	2.4	0.47	0.037	26	70
				Spirogyra sp.	2.1	0.49	0.032	23	66
3	11	0.05	3	*Oedogonium* sp.	4.3	0.4	0.029	33	64
				Ulothrix sp.	5.5	0.38	0.030	27	68
				Cladophora sp.	4.7	0.42	0.033	31	66
				Spirogyra sp.	4.4	0.45	0.027	29	62
5	12	0.05	5	*Oedogonium* sp.	3	0.43	0.031	32	67
				Ulothrix sp.	4	0.41	0.032	25	71
				Cladophora sp.	3.2	0.45	0.034	30	69
				Spirogyra sp.	2.9	0.48	0.029	27	65
2	13	0.05	5	*Oedogonium* sp.	3	0.43	0.031	32	67
				Ulothrix sp.	4	0.41	0.032	25	71
				Cladophora sp.	3.2	0.45	0.034	30	69
				Spirogyra sp.	2.9	0.48	0.029	27	65

3.4. The Effect of Silver Nanoparticles on the Carbohydrates

Carbohydrate accumulation was increased from 0.15 to 0.49 mg/g in *Oedogonium* sp., 0.14 to 0.47 mg/g in *Ulothrix* sp., 0.17 to 0.51 mg/g in *Cladophora* sp., and 0.20 to 0.54 mg/g in *Spirogyra* sp. at 0.08 mg/L of AgNPs at day 7. A larger accumulation of carbohydrates triggers an upsurge in respiration and greater consumption of carbohydrates for the production of energy [24]. The reduction in photosynthetic efficiency under high NP stress inhibits carbohydrate transport, causing the accumulation of starch or sucrose. In order to reduce ionic toxicity, algal cells stimulate glycolysis to reduce the carbohydrates, increase respiration and generate glycerol [25]. Carbon with ATP from glycolysis can also be utilized to produce lipids and energy-intensive mechanisms to improve survival under NP application. Cellular carbon flow supports the production of lipids instead of carbohydrates, as seen in a rise in algal species [26]. In another study, carbohydrates were significantly affected by 24 h of AgNPs in *P. malhamensis* [27]. Silver nanoparticles (90 to 1440 µg/L) increased carbohydrate production to 22 to 80% in *Chlorella* sp. [28]. An increase in carbohydrates is an adaptive response to NP stress that serves as an osmotic agent to enhance absorbency and retain a stability of water metabolism in algal species [29]. Silver nanoparticles increased carbohydrate yield in *Chlorella* sp. by 15% [25]. Accumulation of carbohydrates as storage molecules to protect algal cells was also reported with TiO_2 nanoparticles, which doubled the carbohydrate concentration from controls in *Chlorella sorokiniana* [30] or silver nanoparticles in *Skeletonema costatum* [8].

3.5. Effect of Silver Nanoparticles on Proteins

The protein content improved from 0.019 to 0.038 mg/g in *Oedogonium* sp., 0.020 to 0.039 in *Ulothrix* sp., 0.022 to 0.042 mg/g in *Cladophora* sp., and 0.017 to 0.036 mg/g in *Spirogyra* sp. at 0.08 mg/L of AgNPs at day 7. The accumulation of protein in algae is associated with eliminating toxic effects caused by nanoparticles. Silver has a strong affinity to the sulfur groups that are in many proteins. Methionine and cysteine are sulfur-containing amino acids; therefore, the accumulation of protein in response to nanoparticles is related to a detoxification mechanism preventing algae cells from being damaged in response to NP stress [31]. Antioxidant enzymes and molecular chaperones play a vigorous role in these protective mechanisms. The metalloproteins (metallopeptidases) and phytochelatins (zinc, copper and iron) assist in protecting against the toxicity of NPs. Metalloproteins remove free radicals and serve as a shielding agent to defend algal cells from oxidative stress [32]. Mitogen-activated protein kinases (MAPK) are signaling molecules involved in transmitting information from sensors to cellular responses. ROS production against AgNP stress stimulates the MAPK pathway, down-regulating ROS generation [33].

Moreover, the intracellular augmentation of glutathione occurs to detoxify silver toxicity. Silver toxicity increases the amount of glutathione acting as a precursor of phytochelatins, which assists the mitogen-activated protein kinases pathway function in detoxification [34]. Silver nanoparticles may lyse the algal cell wall to excrete biomolecules such as proteins. Fe_2O_3 NPs at <20 mg/L promoted protein levels in *Scenedesmus obliquus* [22]. Zinc oxide NPs increased the protein accumulation by 1.68 times compared to controls in *Chlorella* sp. [35]. ZnO and Fe_2O_3 NPs increased the protein content in *N. oculata* because these algae produced proteins to detoxify themselves from the toxicity of AgNPs [36].

3.6. Effect of Silver Nanoparticles on Chlorophyll

The chlorophyll was decreased from 40 to 19 µg/gfw in *Oedogonium* sp., 34 to 13 µg/gfw in *Ulothrix* sp., 38 to 17 µg/gfw in *Cladophora* sp., and 35 to 15 µg/gfw in *Spirogyra* sp. at 0.08 mg/L of AgNPs at day 7. The possible reason for the chlorophyll reduction is linked with the sensitivity of the photosynthetic machinery of green algae due to silver ions, as Ag^+ can replace Cu^+ from thiols of functional proteins, leading to the disruption or inactivation of photosynthetic electron transport and photosystem activity [37]. Silver ions ruin photosynthesis in *C. reinhardtii*, disturbing its photosynthetic activity. High concentrations of AgNPs significantly reduce the photosynthetic yield in Isochrysis gal-

bana, as present research indicates; by increasing the application of AgNPs from 0.02 to 0.08 mg/L, the chlorophyll content reduced drastically in all tested algal strains [38]. The photosynthetic performance was highly affected by AgNPs in *Poterioochromonas* malhamensis after 24 h exposure, but in the present study, the photosynthetic performance was highly affected after two days as the algal culture was observed to be green [27]. In one study, Fe_2O_3 NPs reduced the chlorophyll content in *Scenedesmus obliquus* on day 7 at 40 mg/L [39]. The reduction in chlorophyll is associated with the aggregation of NPs, which hinders the pigments from absorbing light and ultimately inhibits photosynthesis [40]. Gold nanoparticles reduced the production of chlorophyll after 72 h of exposure in *C. reinhardtii* and *P. tricornutum*, while Cr_2O_3 changed the PSII energy transfer of *C. reinhardtii* [41]. In one study, Al_2O_3 NPs may have formed aggregates on the cell wall of *Scenedesmus* sp., which might negatively affect the photosynthesis rate and respiration. In addition, dissolved silver ions also directly damaged photosynthetic machinery by adhering to the cell membrane, then penetrating and causing changes in the integrity of the membrane system [18].

3.7. Effect of Silver Nanoparticles on Lipids

The lipid content enlarged from 46 to 74% in *Oedogonium* sp., 50 to 78% in *Ulothrix* sp., 48 to 76% in *Cladophora* sp., and 44 to 72% in *Spirogyra* sp. at 0.08 mg/L of AgNPs at day 7. As the concentration of AgNPs increased, the lipid content also increased in all algae strains under observation. Low doses of NPs enhanced the production of lipids in algae. The toxic metal ion release into the algal cells alters the algal cells, which is reduced by lipid production as a protective mechanism. Lipid induction consequently amends the physiological state of cells by reducing cell wall integrity and cytoplasm shrinkage [42]. AgNPs stimulate Acetyl-coenzyme A carboxylase to catalyze the fatty acid biosynthesis, increasing lipid synthesis. The cellular lipid content acts as an electron sink of ROS to improve the preservation of cellular redox homeostasis and alleviate possible oxidative damage caused by AgNPs [28]. In one study, the lipid content significantly increased from 24 h exposure of AgNPs to *Poterioochromonas* malhamensis [43] because under AgNP stress, malonyl-ACP enters the fatty acid synthesis pathway where β-ketoacyl ACP synthase located on cell membrane catalyzes the condensation reactions to accumulate fatty acids, as found in the current study [44]. The lipid content was improved by 27.8, 32.2, and 53.4 in *Scenedesmus obliquus* by MgO NPs at 0.8, 40, and 100 mg/L, respectively, because algae accumulate lipids as an energy source in response to stress [22]. Similar findings were reported with silicon NPs at 150 mg/L, which increased the lipid content up to 40.26% in *Scenedesmus* sp. [45]. Nanoscale zero-valence iron enhanced lipid content up to 41.90% in *Tetraselmis suecica* and 46.34% in *Pavlova lutheri* [46]. In *Chlorella fusca* the lipid increased by 10.9 and 16.7% with 0.3 and 0.5 g/L of nanofibers, correspondingly [47]. The application of nanoparticles enhanced the lipid yield in many in *Chlorella vulgaris* [25]. Interestingly, in the present study, the increase in lipid was substantial in lipid production compared to other algal species.

3.8. Analysis of Variance (ANOVA)

A lack of fit and an ANOVA test were applied to analyze the significance, reliability and fitness of the model. Results are shown in Supplementary Tables S2–S25. All the models show a p-value < 0.05, indicating that all models were highly substantial, reliable and a good fit for present experimental data.

3.9. Fit Statistic

R^2 is the correlation coefficient that indicates whether the experimental data fit the model. R^2 must be at least 0.80. In all the models, R^2 was greater than 0.8 (Table 3), indicating good compatibility between the actual and calculated results within the range of the experiments.

Table 3. Fit statistics of models.

Algae	Variable	R^2	Adjusted R^2	Adeq Precision	Std. Dev.	Mean	C.V. %
Oedogonium sp.	Growth	0.9862	0.9763	35.5425	0.1364	3.21	4.25
	Carbohydrates	0.9980	0.9965	67.2033	0.0076	0.3615	2.09
	Proteins	0.9993	0.9989	151.171	0.0002	0.0295	0.61
	Chlorophyll	0.9925	0.9872	45.9952	0.6074	30.54	1.99
	Lipids	0.9811	0.9676	24.4970	1.57	61.69	2.55
Ulothrix sp.	Growth	0.9956	0.9924	64.6544	0.0819	4.15	1.97
	Carbohydrates	0.9974	0.9955	58.3222	0.0085	0.3423	2.50
	Proteins	0.9993	0.9989	0.0002	0.0305	151.17	0.59
	Chlorophyll	0.9950	0.9914	58.4744	0.4830	23.92	2.02
	Lipids	0.9842	0.9728	26.4956	1.45	65.62	2.21
Cladophora sp.	Growth	0.9743	0.9560	26.7868	0.2364	3.42	6.90
	Carbohydrates	0.9980	0.9965	67.2033	0.0076	0.3815	1.98
	Proteins	0.9946	0.9907	51.6865	0.0005	0.0325	1.67
	Chlorophyll	0.9925	0.9872	45.9952	0.6074	28.54	2.13
	Lipids	0.9842	0.9728	26.4956	1.45	63.62	2.28
Spirogyra sp.	Growth	0.9966	0.9942	74.2051	0.0730	3.08	2.37
	Carbohydrates	0.9996	0.9993	146.2298	0.0034	0.4085	0.84
	Proteins	0.9993	0.9989	151.1711	0.0002	0.0275	0.6632
	Chlorophyll	0.9950	0.9914	58.4744	0.4830	25.92	1.86
	Lipids	0.9833	0.9713	25.8908	1.49	59.62	2.51

3.10. Equations in Terms of the Coded Equation

In Table S25, the growth, carbohydrates, proteins, chlorophyll and lipids in the algal samples were responses, and A and B were the coded terms of the investigated parameters. A is AgNP concentration, and B is days (duration of silver nanoparticles). These equations can accurately describe the interactions, factors and responses.

3.11. Validity of Models

The standard probability plot of the residuals illustrates the adequacy of the model. Figures 1–4 illustrate the plots of the residuals versus the predictive values of the responses of tested algae. The residuals should fall close to the diagonal reference line [48]. Deviation from this straight line means the residuals were fleeing from normality. All models were well-fitted with the experimental results because residuals from the fitted model were close to the diagonal line and seemed to be normally distributed [49]. The actual values and predicted values in Figures 1–4 are very close to the zero-error line (straight line), which shows the strong correlation between the process factors and the responses to obtain a sustainable model for the algae.

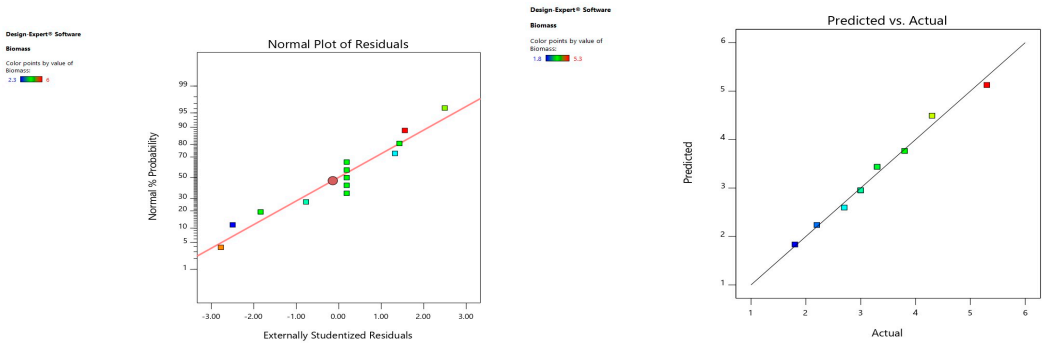

Normal probability plot and studentized residual plot Actual and predicted plots

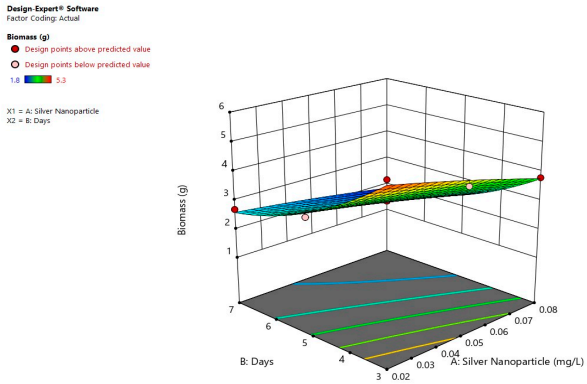

Response surface plots

(**a**)

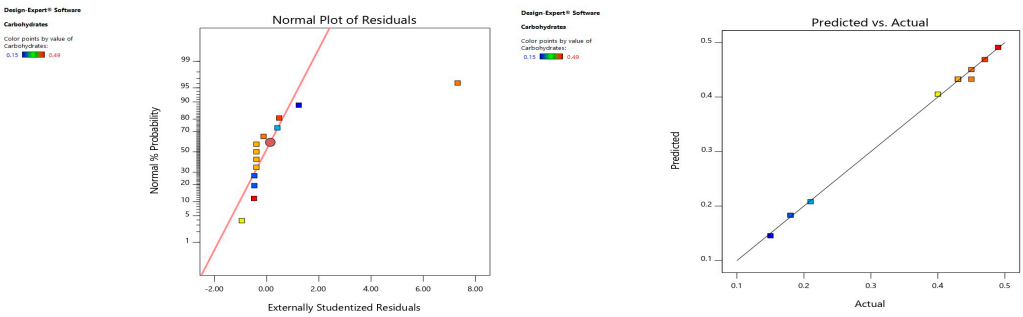

Normal probability plot and studentized residual plot Actual and predicted plots

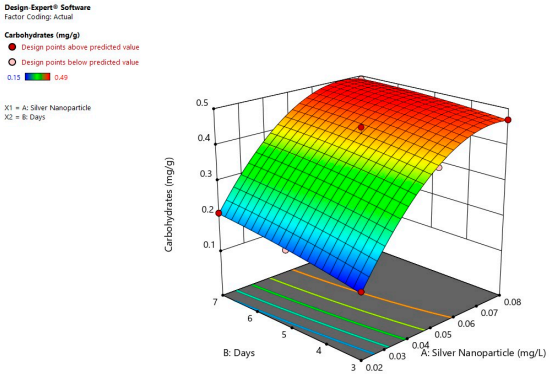

Response surface plots

(**b**)

Figure 1. *Cont.*

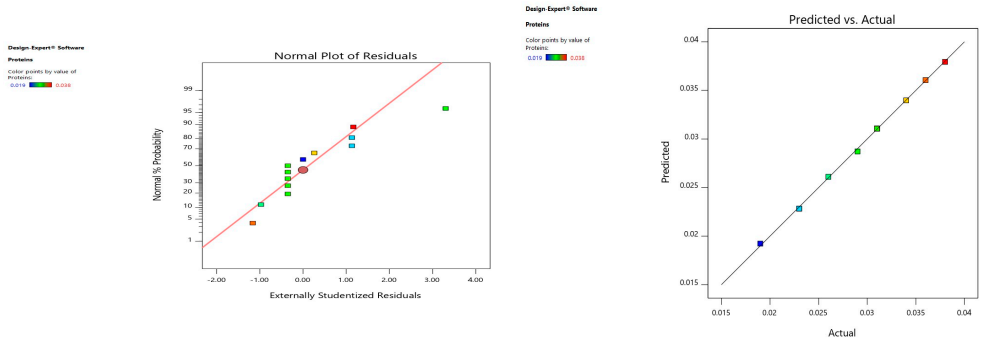

Normal probability plot and studentized residual plot

Actual and predicted plots

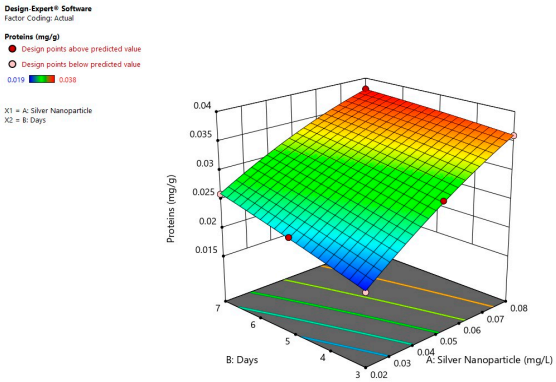

Response surface plots

(**c**)

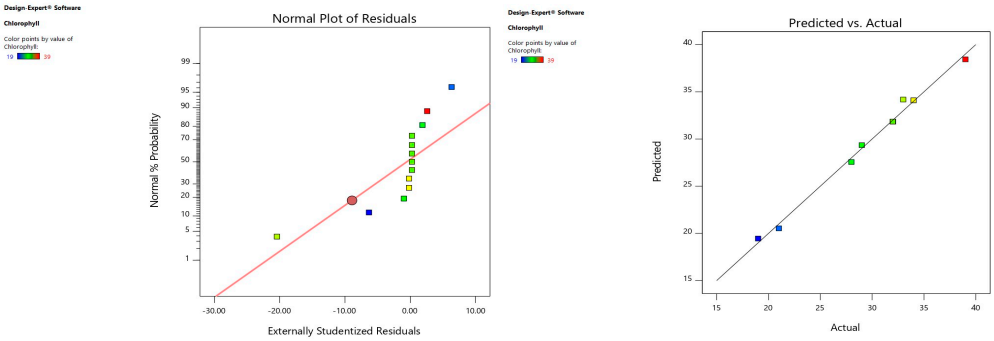

Normal probability plot and studentized residual plot

Actual and predicted plots

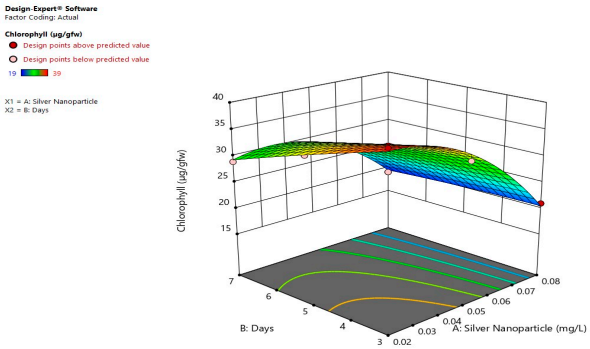

Response surface plots

(**d**)

Figure 1. *Cont.*

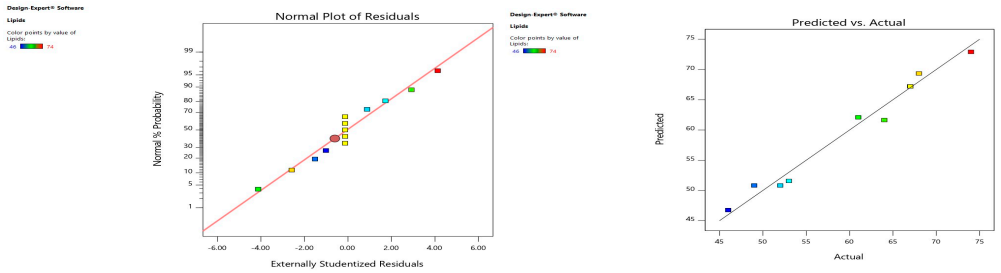

Normal probability plot and studentized residual plot Actual and predicted plots

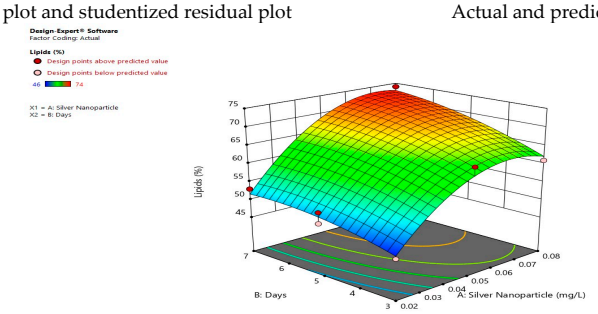

Response surface plots
(**e**)

Figure 1. Response surface plots of (**a**) growth, (**b**) carbohydrates, (**c**) proteins, (**d**) chlorophyll and (**e**) lipids in *Oedogonium* sp. Color based on response value, as blue color shows the minimum points and red color shows the maximum points, pink color indicates points below predicted value.

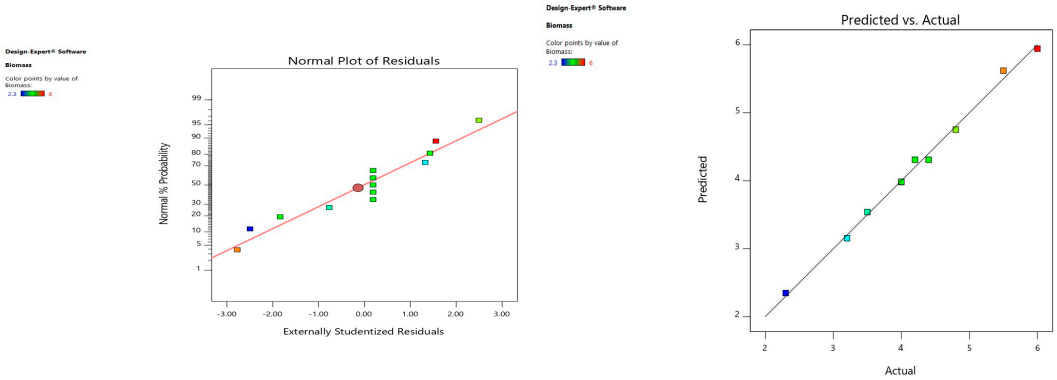

Normal probability plot and studentized residual plot Actual and predicted plots

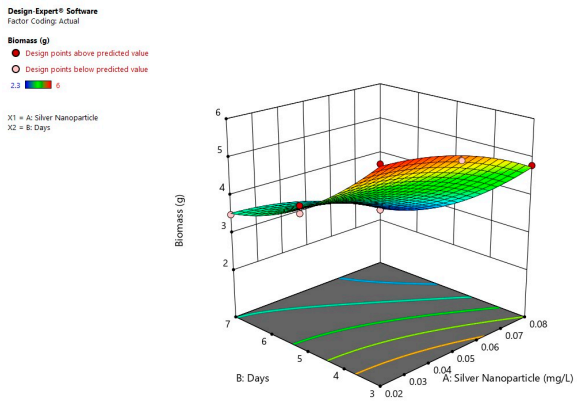

Response surface plots
(**a**)

Figure 2. *Cont.*

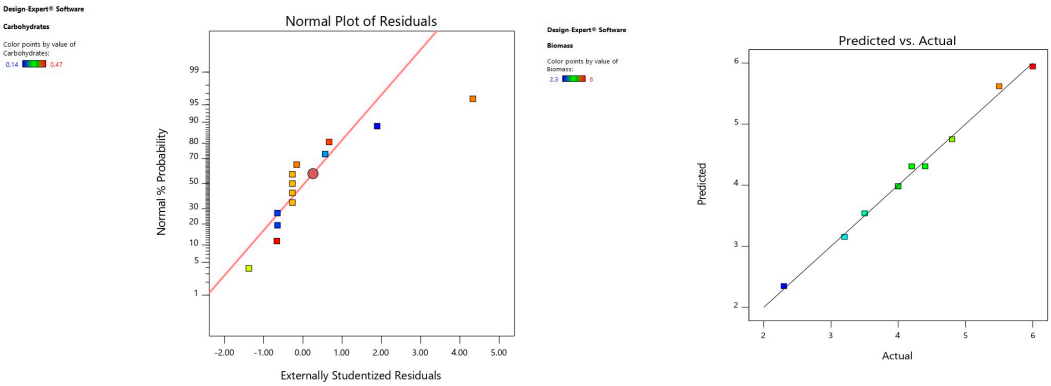

Normal probability plot and studentized residual plot Actual and predicted plots

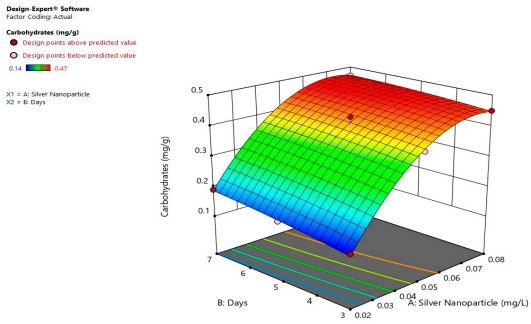

Response surface plots

(**b**)

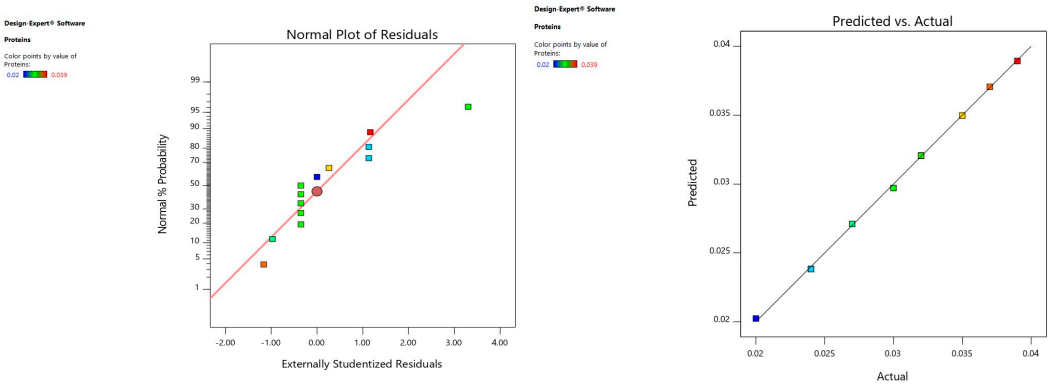

Normal probability plot and studentized residual plot Actual and predicted plots

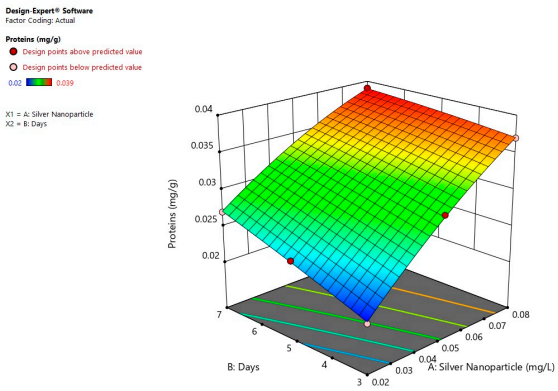

Response surface plots

(**c**)

Figure 2. *Cont*.

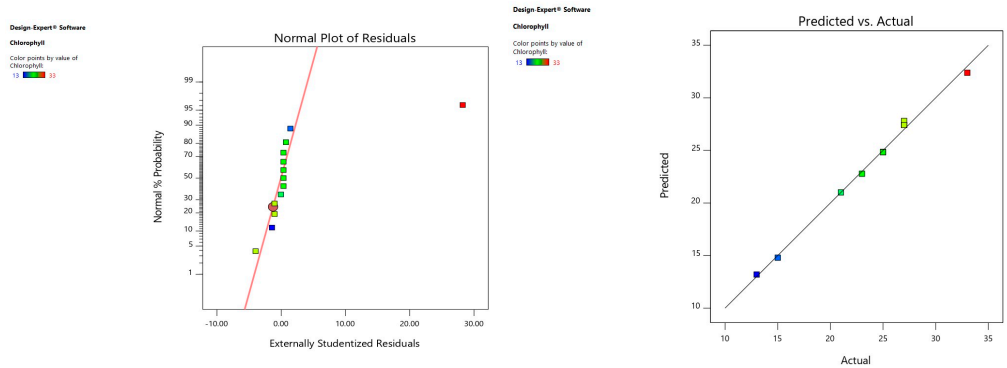

Normal probability plot and studentized residual plot

Actual and predicted plots

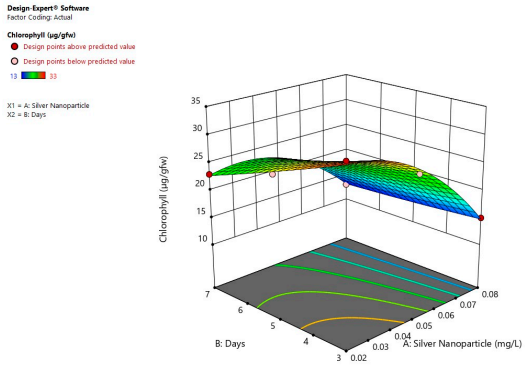

Response surface plots
(**d**)

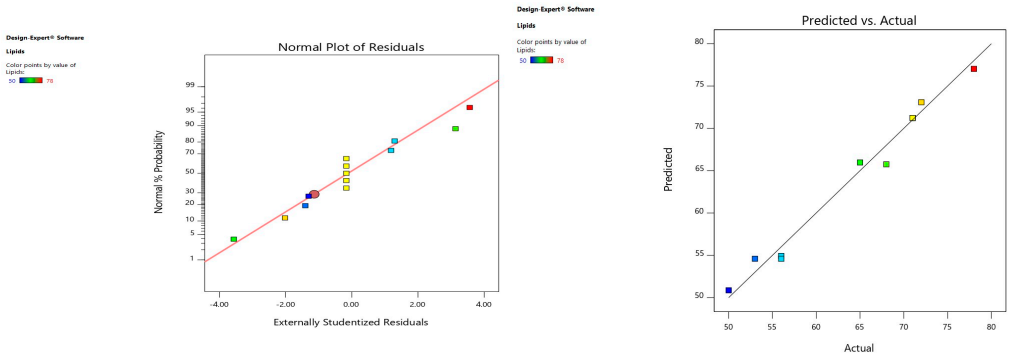

Normal probability plot and studentized residual plot

Actual and predicted plots

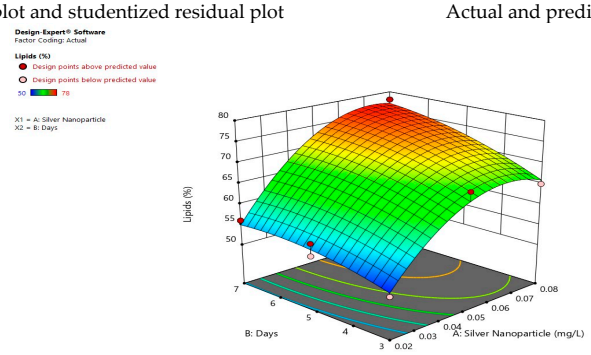

Response surface plots
(**e**)

Figure 2. Response surface plots of (**a**) growth, (**b**) carbohydrates, (**c**) proteins, (**d**) chlorophyll and (**e**) lipids in *Ulothrix* sp. Color based on response value, as blue color shows the minimum points and red color shows the maximum points, pink color indicates points below predicted value.

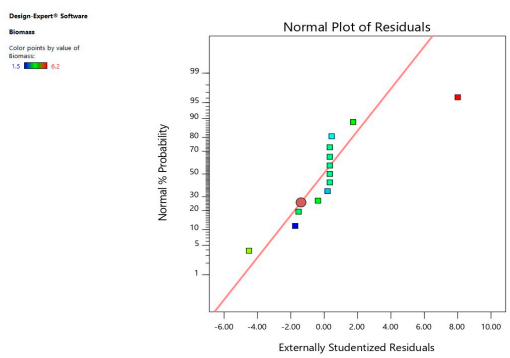

Normal probability plot and studentized residual plot

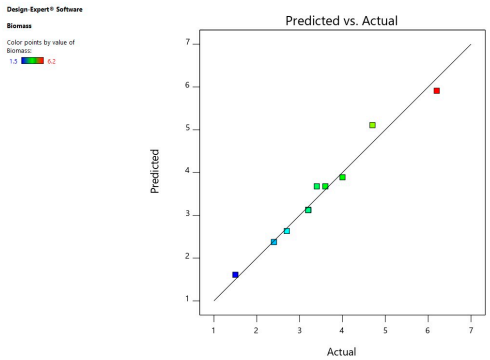

Actual and predicted plots

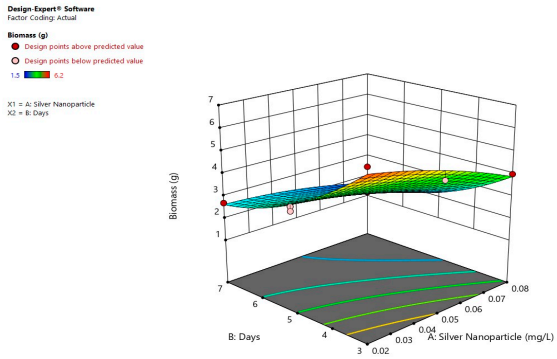

Response surface plots

(**a**)

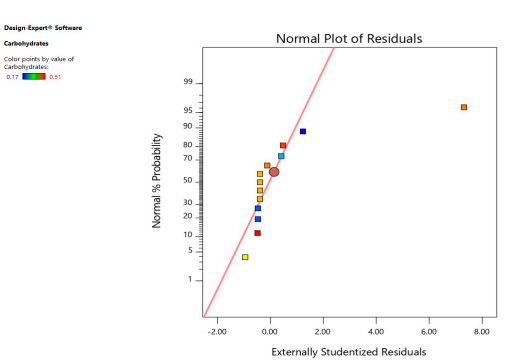

Normal probability plot and studentized residual plot

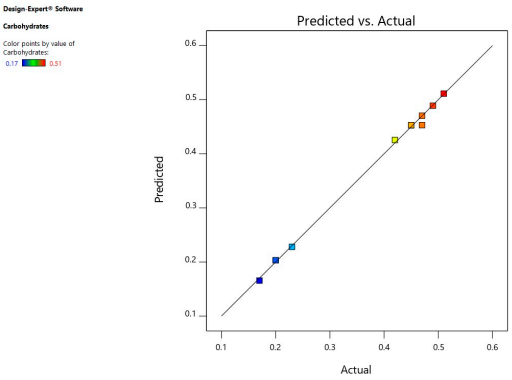

Actual and predicted plots

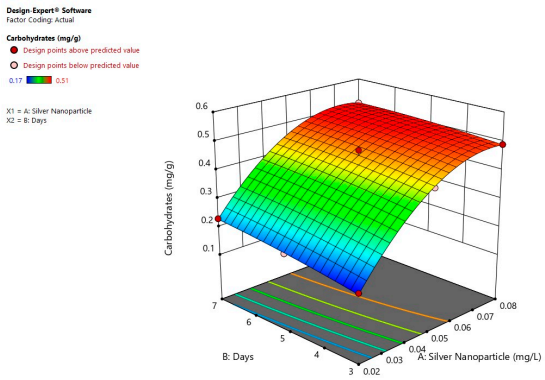

Response surface plots

(**b**)

Figure 3. *Cont.*

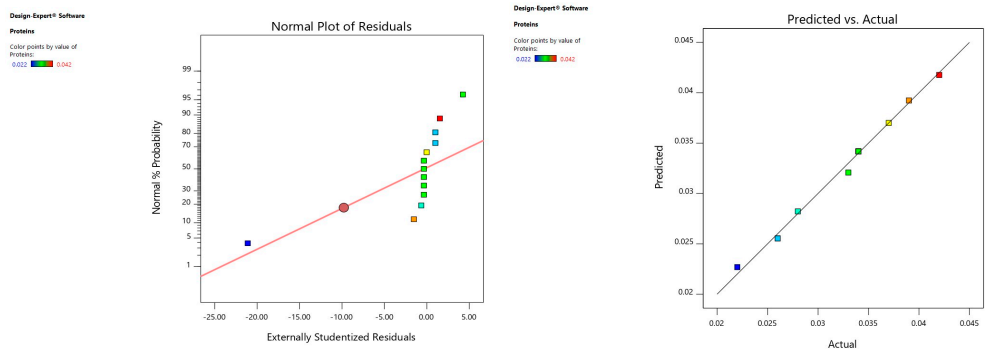

Normal probability plot and studentized residual plot Actual and predicted plots

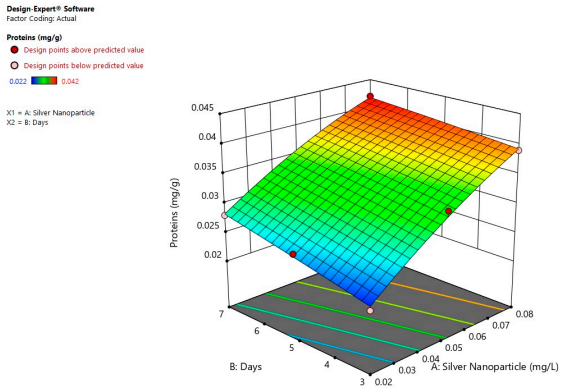

Response surface plots

(**c**)

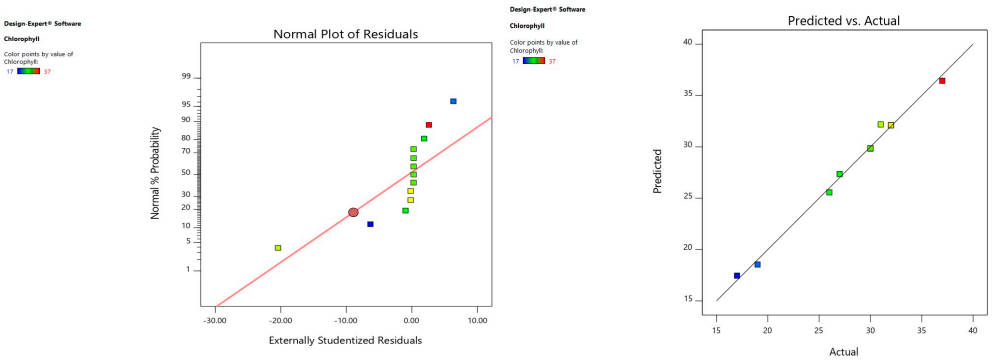

Normal probability plot and studentized residual plot Actual and predicted plots

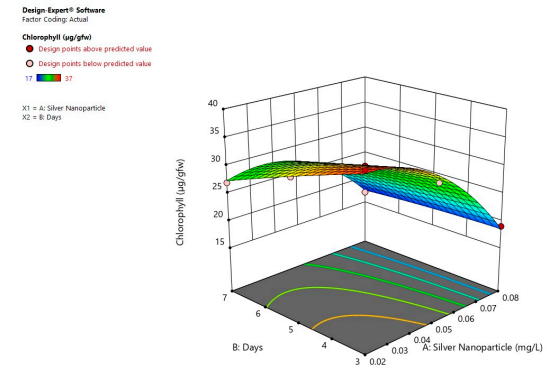

Response surface plots

(**d**)

Figure 3. *Cont.*

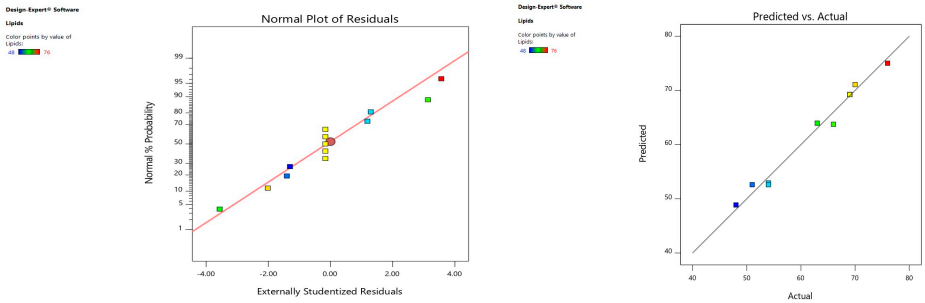

Normal probability plot and studentized residual plot

Actual and predicted plots

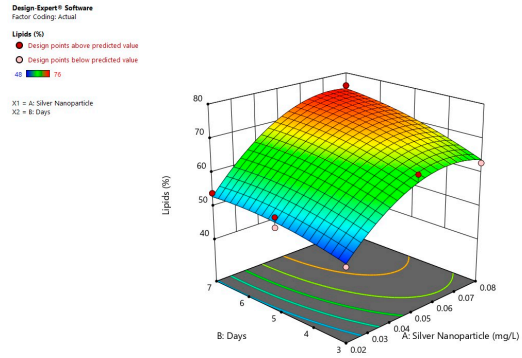

Response surface plots
(**e**)

Figure 3. Response surface plots of (**a**) growth, (**b**) carbohydrates, (**c**) proteins, (**d**) chlorophyll and (**e**) lipids in *Cladophora* sp. Color based on response value, as blue color shows the minimum points and red color shows the maximum points, pink color indicates points below predicted value.

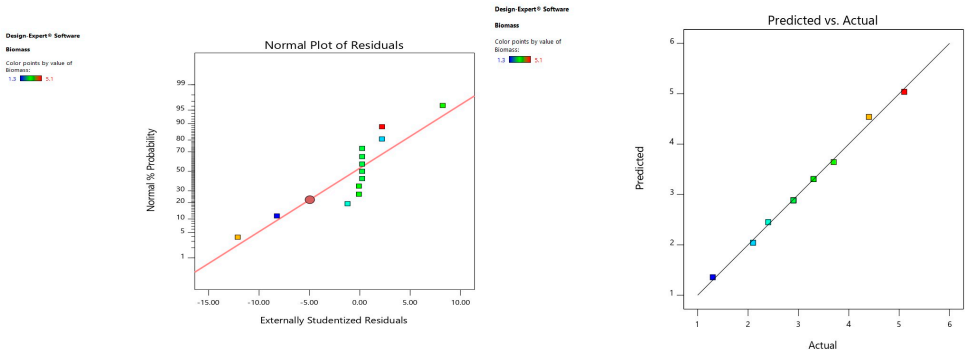

Normal probability plot and studentized residual plot

Actual and predicted plots

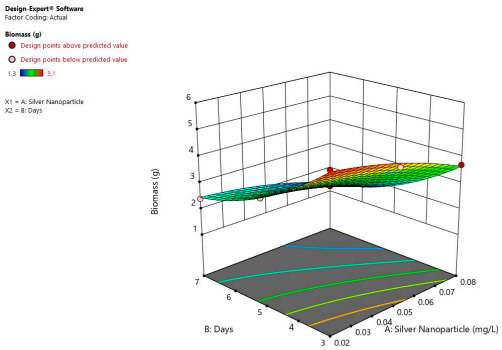

Response surface plots
(**a**)

Figure 4. *Cont.*

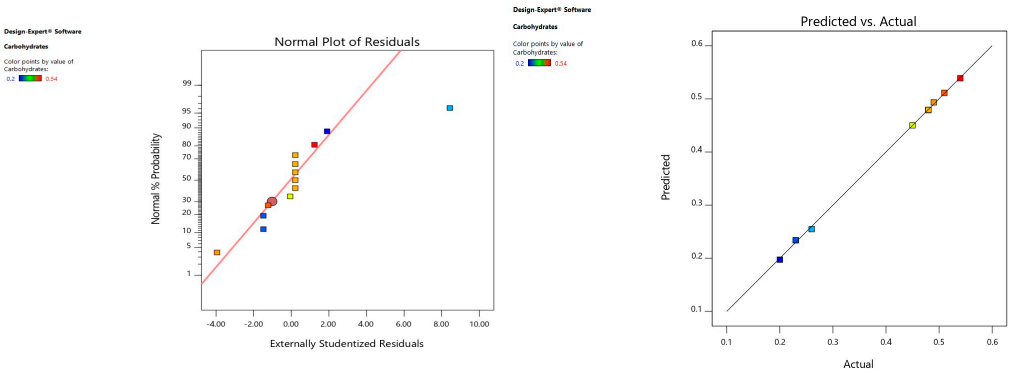

Normal probability plot and studentized residual plot Actual and predicted plots

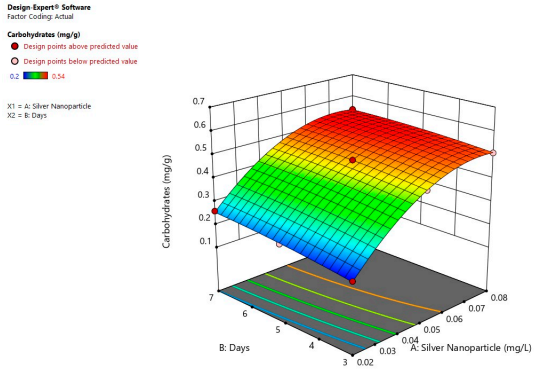

Response surface plots

(**b**)

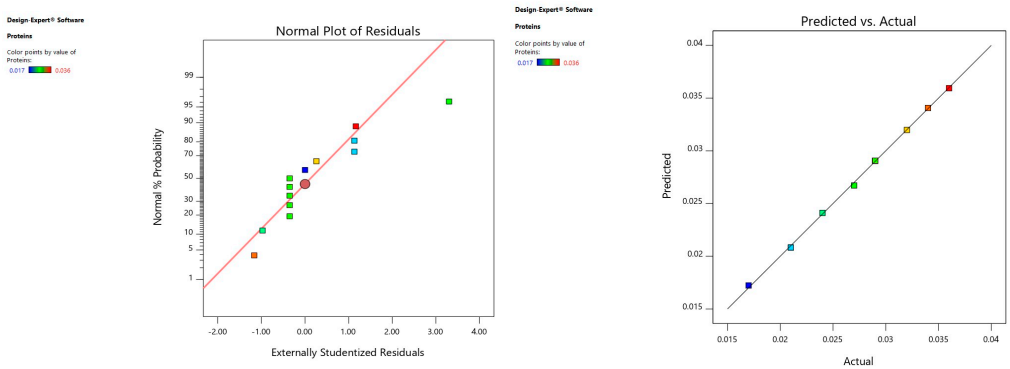

Normal probability plot and studentized residual plot Actual and predicted plots

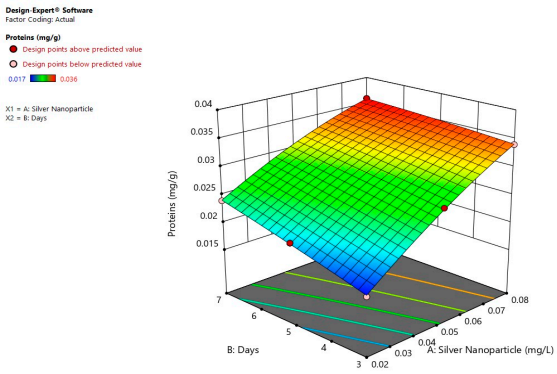

Response surface plots

(**c**)

Figure 4. *Cont*.

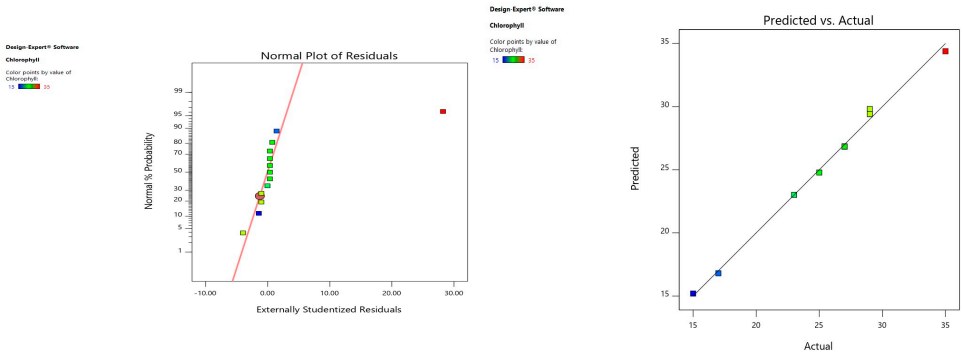

Normal probability plot and studentized residual plot Actual and predicted plots

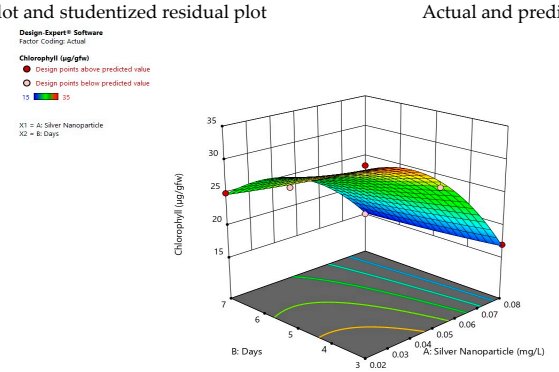

Response surface plots
(**d**)

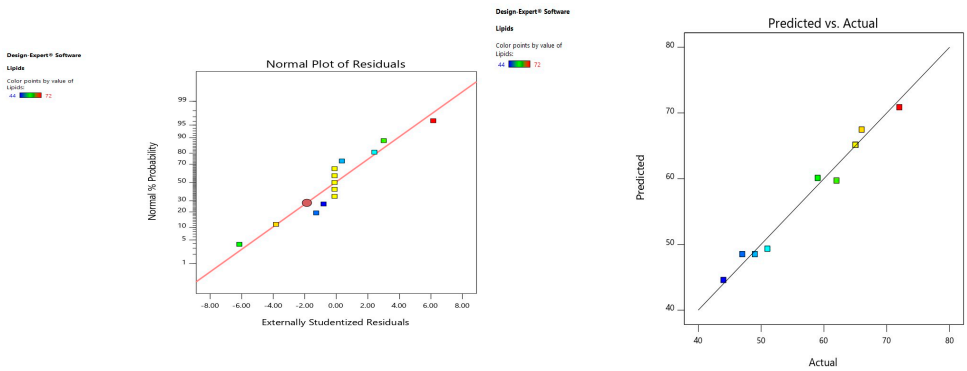

Normal probability plot and studentized residual plot Actual and predicted plots

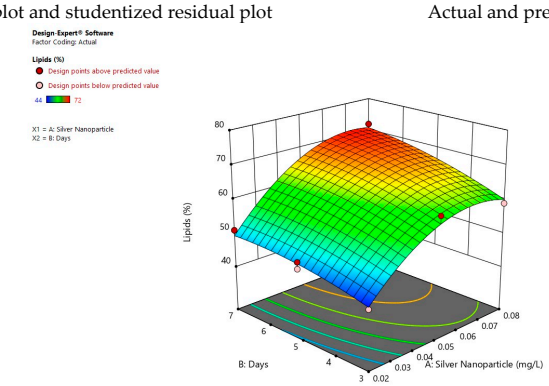

Response surface plots
(**e**)

Figure 4. Response surface plots of (**a**) growth, (**b**) carbohydrates, (**c**) proteins, (**d**) chlorophyll and (**e**) lipids in *Spirogyra* sp. Color based on response value, as blue color shows the minimum points and red color shows the maximum points, pink color indicates points below predicted value.

3.12. Interaction of Factors on Response

The effect of the process variable (AgNP concentration and days) on growth, carbohydrates, proteins, chlorophyll and lipids are represented in Figures 1–4. Algal growth and chlorophyll were observed to decrease with increases in the concentration of AgNPs concerning days, while carbohydrates, proteins and lipids were observed to increase with increases in the concentration of AgNPs with respect to days. Three-dimensional plots provide a visualization of the relationship between the response and interaction between operating variables to optimize conditions for adding AgNPs in algal cultures. The three-dimensional plots demonstrate the optimal level of each parameter for maximum response. Figures 1–4 manage two variables at their zero level at a time. The maximum predicted value relies on two variables at a time. Algal growth and chlorophyll were observed to decrease with increases in the concentration of AgNPs with respect to days, while carbohydrates, proteins and lipids were observed to increase with increases in the concentration of AgNPs with respect to days. The trends were the same in all four species.

3.13. Fatty Acid Profile via GCMS

In experimental run 6, with 0.08 mg/g at day 7, the highest lipid content was obtained in all tested algal strains, which were further analyzed via GCMS for fuel property evaluation. The fatty acid profile of *Oedogonium* sp., *Ulothrix* sp., *Cladophora* sp. and *Spirogyra* sp. before and after AgNP stress is shown in Table 4. Under AgNP stress, 16 fatty acids were detected in *Oedogonium* sp., 17 in *Ulothrix* sp., 14 in *Cladophora* sp. and 20 in *Spirogyra* sp. The results demonstrate that after AgNP stress, C14:1 slightly reduced in algal strains except in *Ulothrix* sp. The portions of myristic acid, methyl myristate, methyl palmitoleate, methyl palmitate, linolenate, and linoleate were reduced after AgNP stress in all tested algal strains. Linolenic acid was detected only in *Oedogonium* sp. and *Spirogyra* sp., reduced after AgNPs stress. Hexadecadienoic was detected only in the control of *Oedogonium* sp. and *Spirogyra* sp., while erucic acid in *Oedogonium* sp. and *Cladophora* sp. was not found after AgNP stress. Caprylate, caprate and laureate were detected in *Ulothrix* sp. and *Cladophora sp.*, and remained the same after AgNP stress. Arachidic acid and gondoic acid were increased after AgNP stress only in *Spirogyra* sp. ethyl oleate, palmatic acid and linoleic acid were increased after AgNP stress in all tested algal strains. Stearic acid and palmitoleic acid slightly increased in *Oedogonium* sp. and *Spirogyra* sp. after AgNP stress. After AgNP stress, oleic acid and methyl stearate significantly increased in all algal strains except for *Cladophora* sp., where both fatty acids were absent before and after AgNP stress. Arachidate and erucate were detected in *Ulothrix* sp. and *Cladophora* sp., reduced after AgNP stress. Behenic acid was detected in all tested algal strains after AgNP stress.

In the present study, methyl palmitate was the dominating fatty acid. The results show that the saturated fatty acids and PUFAs increased while MUFAs reduced after contact with 0.08 mg/L AgNPs. A high composition of saturated fatty acids after AgNP treatment suggests that the lipids produced are extra stable and invulnerable to autoxidation in storage. Identical results were reported in *C. vulgaris,* where after 15 mg/L AgNP treatment, the SFAs increased from 54.88 to 61.47% and 52.81 to 67.27% in *D. splendida*. The UFAs decreased from 45.11 to 39% in *C. vulgaris* and 47.18 to 32.73% in *D. splendida*, while MUFAs decreased from 30.99 to 14.33% and 33.57 to 15.75% in *C. vulgaris* and *D. splendida,* respectively [16]. Palmitic acid was 43.06 and 46.57% in *C. vulgaris* and *D. splendida,* respectively. Linoleic acid was 20.62 and 20.12% in *C. vulgaris* and *D. splendida,* respectively [24]. The fatty acid composition confirms that the exposure of AgNPs alters the metabolism of all the tested algal strains towards the production of hydrocarbons (Figure 5).

Table 4. GC-MS fatty acid profile (% DW) of algal strains before and after AgNP stress.

Fatty Acids	*Oedogonium* sp.		*Ulothrix* sp.		*Cladophora* sp.		*Spirogyra* sp.	
	Control	AgNPs Stress	Control	AgNPs Stress	Control	AgNPs Stress	Control	AgNPs Stress
Myristoleic acid (14:1)	0.18	0.15	-	-	0.34	0.31	0.18	0.17
Myristic acid (14:0)	0.36	0.35	0.17	0.15	0.16	0.14	0.09	0.07
Hexadecadienoic (16:2)	0.48	-	-	-	-	-	2.26	-
Palmitoleic acid (16:1)	2.97	3.10	-	-	-	-	0.32	0.35
Palmatic acid (16:0)	1.16	2.5	0.26	1.01	0.44	0.50	0.11	0.21
Linolenic acid (18:3)	0.46	0.21	-		-	-	0.68	0.31
Linoleic acid (18:2)	0.37	0.39	0.50	0.48	2.07	2.05	1.09	1.01
Oleic acid (18:1)	3.14	3.21	0.45	0.50	-	-	0.39	0.45
Stearic acid (18:0)	1.33	1.38	-	-	-	-	0.10	0.19
Gondoic acid (20:1)	-	-	-	-	-	-	0.19	0.21
Arachidic acid (20:0)	-	-	-	-	-	-	0.19	0.23
Erucic acid (22:1)	0.41	-	-	-	0.14	-	-	-
Caprylate (8:0)	-	-	0.35	0.35	0.36	0.36	-	-
Caprate (10:0)	-	-	0.63	0.63	0.12	0.12	-	-
Laurate (12:0)	-	-	0.23	0.23	0.61	0.60	-	-
Methyl myristate (14:0)	4.54	4.12	3.35	1.90	3.35	2.13	2.54	2.10
Methyl palmitoleate (16:1)	3.15	2.92	5.12	3.01	3.24	3.01	6.10	5.91
Methyl palmitate (16:0)	46.4	44.2	24.6	21.0	34.3	32.1	49.9	48.0
Linolenate (18:3)	2.33	2.01	2.64	1.81	7.60	6.10	1.19	1.10
Linoleate (18:2)	2.52	1.91	9.12	6.21	5.41	4.51	0.58	0.23
Methyl oleate (18:1)	28.1	26.01	44.5	37.1	42.2	33.1	29.9	28.0
Methyl stearate (18:0)	2.12	1.92	3.83	2.21	-	-	5.43	4.23
Arachidate (21:0)	-	-	2.43	2.21	-	-	1.17	1.01
Erucate (22:1)	-	-	2.23	1.72	-	-	0.58	0.43
Behenic acid (22:0)	-	0.09	-	0.07	-	0.10	-	0.14

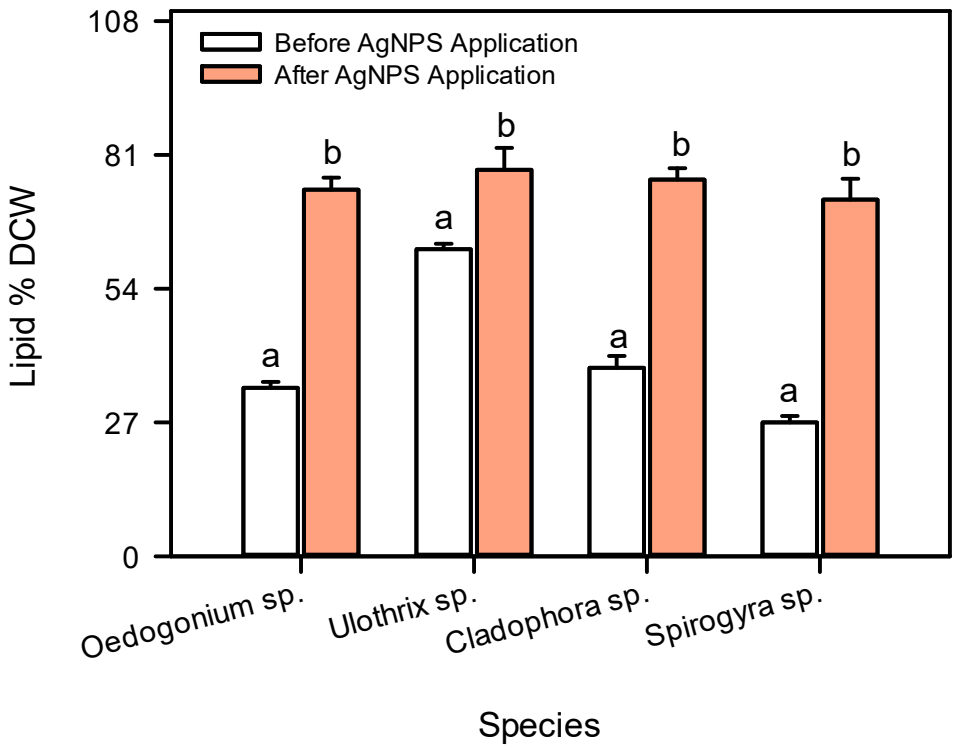

Figure 5. Lipid production yield in studied algal species before and after silver nanoparticle application. (Different letters show different letters indicate significant difference at $p = 0.05$ according to Duncan's new multiple range test).

3.14. Algal Fuel Properties

Biodiesel properties before and after the application of AgNPs are presented in Table 5. The results indicate that IV was reduced from 110 to 102 g I_2/100 g in *Oedogonium* sp., 114 to 89 g I_2/100 g in *Ulothrix* sp., 122 to 103 g I_2/100 g in *Cladophora* sp., and 109 to 104 g I_2/100 g in *Spirogyra* sp. after exposure to AgNPs. According to EN 14214, biodiesel

should have an IV less than 120 g I_2/100 g, while no specifications have been reported in the ASTM D6751. The IV is under 120 g I_2/100 g in the present study in all tested algal strains. The lowest IV was calculated in *Ulothrix* sp. after exposure to AgNPs. Table 5 shows that under treatment with AgNPs, the saponification value reduced from 202 to 191 mg KOH/g in Oedogonium sp., 197 to 158 mg KOH/g in *Ulothrix* sp., 199 to 170 mg KOH/g in *Cladophora* sp., and 206 to 189 mg KOH/g in *Spirogyra* sp. No specification for SV has been reported in standards, with the lowest SV noted in *Ulothrix* sp. after treatment with AgNPs. The cetane number is the vital parameter in determining the combustion quality of biodiesel. Table 5 shows that after treatment with AgNPs, the cetane number increased from 48.6 to 53 in *Oedogonium* sp., 48.5 to 61 in *Ulothrix* sp., 47 to 56 in *Cladophora* sp., and 48 to 52.6 in *Spirogyra* sp. In accordance with ASTM D6751, the cetane number should be a minimum of 48 and 52 in the EN 14214. In the present study, the cetane number in all algal strains was greater than 47. These results indicate that the CN in all algal strains increased after the treatment with AgNPs, with the highest CN recorded in *Ulothrix* sp. after treatment with AgNPs.

Table 5. Biodiesel properties of algal strains under silver nanoparticle stress.

Algae		IV (g $I_2$100/g fat)	SV (mg KOH/g)	CN	LCSF	CFPP (°C)	HHV*i* (MJ/kg)	P (g cm^{-3})	υ (mm^2/s)	Y at 110 °C (Hour)
Biodiesel Standard EN 14214		≤120	-	≥51	-	≤5/≤−20	-	0.86–0.9	3.5–5.0	≥ 6
Biodiesel Standard ASTM D6751-02		-	-	≥47	-	-	-	-	1.9–6.0	-
Oedogonium sp.	Control	110	202	48.6	0.77	−14.03	38.4	0.87	3.6	114
	AgNPs Stress	102	191	53	0.94	−13.52	39.5	0.88	3.6	199
Ulothrix sp.	Control	114	197	48.5	0.026	−16.39	39.3	0.88	3.7	238
	AgNPs Stress	89	158	61	0.101	−16.15	40	0.88	3.8	248
Cladophora sp.	Control	122	199	47	0.04	−16.47	36	0.86	3.7	59
	AgNPs Stress	103	170	56	0.05	−16.31	39	0.88	3.8	61
Spirogyra sp.	Control	109	206	49	0.25	−15.68	37	0.86	3.5	82
	AgNPs Stress	104	189	52	0.34	−15.38	38	0.87	3.6	84

In current findings, the HHV was in the range of 36 to 40 MJ/kg. According to the ASTM standard, a high heating value for biodiesel should be more than 35 MJ/kg, while no specifications have been reported in the EN 14214 [50]. After treatment with AgNPs, the HHV increased compared to the controls. The highest HHV was noted in *Ulothrix* sp. after treatment with AgNPs. To determine biodiesel flow performance at low temperatures, the cold filter plugging point was used [51]. In the present study, the CFPP of all four algal species was −13.52 to −16.47 °C. According to EN 14214, the CFPP of biodiesel should be ≤5/≤−20 °C, while there is no specification for CFPP in the ASTM 6751. CFPP is interrelated with the LCSF. Biodiesel possessing a significant fraction of C18:0 and C16:0 attains higher CFPP [52]. The results indicate that the kinematic viscosity of tested algal strains was 3.5 to 3.8 mm^2 s $^{-1}$, which is in the range of both standards ASTM 6751 (1.9–6.0 mm^2 s $^{-1}$) and EN 14214 (3.5–5.0 mm^2 s $^{-1}$). The density of the biodiesel fuel for all four algae strains was in the range of 0.86 to 0.88 g cm^{-3}. According to the EN 14214, the density of biodiesel should be between 0.86 and 0.9 g cm^{-3}, while there is no specification for density in the ASTM 6751. To ensure the storage of biodiesel without autoxidation, biodiesel must have suitable oxidation stability at 110 °C. Oxidation stability should ≥6 h at 110 °C (EN 14214), while no specification is recorded in the ASTM 6751 [53]. The results indicate that the overall oxidation stability of the biodiesel fuel for all four algae strains is in the range of 46 to 382 h. The oxidation stability increased in *Oedogonium* sp. from 114 to 199 h and in *Ulothrix* sp. to 238 h after treatment with AgNPs. The highest oxidation stability was noted in *Ulothrix* sp. after AgNP stress (0.08 mg/L). *Oedogonium* sp., *Ulothrix* sp., *Cladophora* sp. and *Spirogyra* sp. were subjected to AgNP stress to enhance lipid production and improve FAMEs composition for fuel production. All fuel properties in tested algal strains after treatment with AgNPs were within the range of standards [54].

4. Conclusions

The current study provides a reliable method to clean water with valuable byproducts and biodiesel production by using local algae. The application of NPs to the cultures of algae is an effective substitute to increase the enrichment and production of biodiesel from non-conventional resources. This study demonstrates that the production of carbohydrates, proteins and lipids was substantially greater after the application of nanoparticles. Carbohydrates in *Oedogonium* sp. were 0.49 mg/g, 0.47 mg/g in *Ulothrix* sp., 0.51 mg/g in *Cladophora* sp. and 0.54 mg/g in *Spirogyra* sp., while proteins were 0.038 mg/g in *Oedogonium* sp., 0.039 mg/g in *Ulothrix* sp., 0.042 mg/g in *Cladophora* sp. and 0.036 mg/g in *Spirogyra* sp. from using 0.08 mg/L of silver nanoparticles applied at day 7. Total lipid increased from 46 to 74% in *Oedogonium* sp., 50 to 78% in *Ulothrix* sp., 48 to 76% in *Cladophora* sp. and 44 to 72% in *Spirogyra* sp. using 0.08 mg/L of silver nanoparticles applied at day 7. The lipids and fatty acid fractions from algae contain high oleic acid, palmitic acid, and stearic acid concentrations. The lipid composition in algal species can be enhanced by applying silver nanoparticles, which have a positive effect on cellular activity in *Oedogonium* sp., *Ulothrix* sp., *Cladophora* sp., and *Spirogyra* sp. The implications of silver nanoparticles are still at an early stage, and substantial research to overcome the barriers to releasing toxic ions and their damage to cellular activity requires further investigation.

Supplementary Materials: The supplementary material is available. The following supporting information can be downloaded at: https://www.mdpi.com/article/10.3390/agriculture13010073/s1, Table S1. BG media Composition; Table S2. ANOVA for Quadratic model of Growth in *Oedogonium* sp.; Table S3. ANOVA for Quadratic model of Carbohydrates in *Oedogonium* sp.; Table S4. ANOVA for Quadratic model of Proteins in *Oedogonium* sp.; Table S5. ANOVA for Quadratic model of Chlorophyll in *Oedogonium* sp.; Table S6. ANOVA for Quadratic model of Lipids in *Oedogonium* sp.; Table S7. ANOVA for Quadratic model of Growth in *Ulothrix* sp.; Table S8. ANOVA for Quadratic model of Carbohydrates in *Ulothrix* sp.; Table S9. ANOVA for Quadratic model of Proteins in *Ulothrix* sp.; Table S10. ANOVA for Quadratic model of Chlorophyll in *Ulothrix* sp.; Table S11. ANOVA for Quadratic model of Lipids in *Ulothrix* sp.; Table S12. ANOVA for Quadratic model of Growth in *Cladophora* sp.; Table S13. ANOVA for Quadratic model of Carbohydrates in *Cladophora* sp.; Table S14. ANOVA for Quadratic model of Proteins in *Cladophora* sp.; Table S15. ANOVA for Quadratic model of Chlorophyll in *Cladophora* sp.; Table S16. ANOVA for Quadratic model of Lipids in *Cladophora* sp.; Table S17. ANOVA for Quadratic model of Growth in Spirogyra sp.; Table S18. ANOVA for Quadratic model of Carbohydrates in *Spirogyra* sp.; Table S19. ANOVA for Quadratic model of Proteins in *Spirogyra* sp.; Table S20. ANOVA for Quadratic model of Chlorophyll in *Spirogyra* sp.; Table S21. ANOVA for Quadratic model of Lipids in *Spirogyra* sp.; Table S22. ANOVA for Quadratic model of AgNPs uptake in *Oedogonium* sp.; Table S23. ANOVA for Quadratic model of AgNPs uptake in *Ulothrix* sp.; Table S24. ANOVA for Quadratic model of AgNPs uptake in *Cladophora* sp.; Table S25. ANOVA for Quadratic model of AgNPs uptake in Spirogyra sp.; Figure S1. Phylogenetic tree using the Neighbor-Joining method.

Author Contributions: Conceptualization, N.M.; methodology, M.H.; formal analysis, Z.A. and F.A.; investigation, M.H.; resources, N.M.; writing—original draft preparation, M.H.; writing—review and editing, D.A.D., R.M. and F.A.; visualization and supervision, N.M.; project administration and funding acquisition, N.M. and R.M. All authors have read and agreed to the published version of the manuscript.

Funding: The present work is supported by Higher Education Commission grant No. (NRPU-2738).

Institutional Review Board Statement: Not applicable.

Informed Consent Statement: Not applicable.

Data Availability Statement: Not applicable.

Conflicts of Interest: The authors declare no conflict of interest.

References

1. Bologna, M.; Aquino, G. Deforestation and World Population Sustainability: A Quantitative Analysis. *Sci. Rep.* **2020**, *10*, 7631. [CrossRef] [PubMed]
2. Hasnain, M.; Munir, N.; Siddiqui, Z.S.; Ali, F.; El-Keblawy, A.; Abideen, Z. Integral Approach for the Evaluation of Sugar Cane Bio-Waste Molasses and Effects on Algal Lipids and Biodiesel Production. *Waste Biomass Valorization* **2022**, 1–20. [CrossRef]
3. Hasnain, M.; Abideen, Z.; Naz, S.; Roessner, U.; Munir, N. Biodiesel Production from New Algal Sources Using Response Surface Methodology and Microwave Application. *Biomass Convers. Biorefinery* **2021**. [CrossRef]
4. Abideen, Z.; Waqif, H.; Munir, N.; El-Keblawy, A.; Hasnain, M.; Radicetti, E.; Mancinelli, R.; Nielsen, B.L.; Haider, G. Algal-Mediated Nanoparticles, Phycochar, and Biofertilizers for Mitigating Abiotic Stresses in Plants: A Review. *Agronomy* **2022**, *12*, 1788. [CrossRef]
5. Munir, N.; Hasnain, M.; Waqif, H.; Adetuyi, B.O.; Egbuna, C.; Olisah, M.C.; Chikwendu, C.J.; Uche, C.Z.; C Patrick-Iwuanyanwu, K.; El Sayed, A.M.A. Gelling Agents, Micro and Nanogels in Food System Applications. In *Application of Nanotechnology in Food Science, Processing and Packaging*; Springer: Berlin/Heidelberg, Germany, 2022; pp. 153–167.
6. Munir, N.; Hasnain, M.; Hanif, M.; Waqif, H.; Sharif, N. Fungal Organisms: A Check for Harmful Algal Blooms. In *Freshwater Mycology*; Elsevier: Amsterdam, The Netherlands, 2022; pp. 91–115.
7. Qidwai, A.; Kumar, R.; Dikshit, A. Green Synthesis of Silver Nanoparticles by Seed of *Phoenix sylvestris* L. and Their Role in the Management of Cosmetics Embarrassment. *Green Chem. Lett. Rev.* **2018**, *11*, 176–188. [CrossRef]
8. Huang, J.; Cheng, J.; Yi, J. Impact of Silver Nanoparticles on Marine Diatom *Skeletonema costatum*. *J. Appl. Toxicol.* **2016**, *36*, 1343–1354. [CrossRef] [PubMed]
9. El-Sheekh, M.M.; Bedaiwy, M.Y.; Osman, M.E.; Ismail, M.M. Influence of Molasses on Growth, Biochemical Composition and Ethanol Production of the Green Algae *Chlorella vulgaris* and *Scenedesmus obliquus*. *J. Agric. Eng. Biotechnol.* **2014**, *2*, 20. [CrossRef]
10. Kumar, D.; Abdul Rub, M.; Akram, M.; Kabir-ud-Din. Interaction of Chromium (III) Complex of Glycylphenylalanine with Ninhydrin in Aqueous and Cetyltrimethylammonium Bromide (CTAB) Micellar Media. *Tenside Surfactants Deterg.* **2014**, *51*, 157–163. [CrossRef]
11. Isaac, R.A.; Kerber, J.D. Atomic Absorption and Flame Photometry: Techniques and Uses in Soil, Plant, and Water Analysis. In *Instrumental Methods for Analysis of Soils and Plant Tissue*; Wiley: Hoboken, NJ, USA, 1971; pp. 17–37.
12. Hasnain, M.; Abideen, Z.; Hashmi, S.; Naz, S.; Munir, N. Assessing the Potential of Nutrient Deficiency for Enhancement of Biodiesel Production in Algal Resources. *Biofuels* **2022**, 1–34. [CrossRef]
13. Lichtenthaler, H.K.; Buschmann, C. Chlorophylls and Carotenoids: Measurement and Characterization by UV-VIS Spectroscopy. *Curr. Protoc. Food Anal. Chem.* **2001**, *1*, F4-3. [CrossRef]
14. Munir, N.; Sharif, N.; Naz, S.; Saleem, F.; Manzoor, F. Harvesting and Processing of Microalgae Biomass Fractions for Biodiesel Production (a Review). *Sci. Technol. Dev.* **2016**, *32*, 235–243.
15. Munir, N.; Hasnain, M.; Sarwar, Z.; Ali, F.; Hessini, K.; Abideen, Z. Changes in Environmental Conditions Are Critical Factors for Optimum Biomass, Lipid Pattern and Biodiesel Production in Algal Biomass. *Biologia* **2022**, *77*, 3099–3124. [CrossRef]
16. Hasnain, M.; Abideen, Z.; Anthony Dias, D.; Naz, S.; Munir, N. Utilization of Saline Water Enhances Lipid Accumulation in Green Microalgae for the Sustainable Production of Biodiesel. *BioEnergy Res.* **2022**, 1–14. [CrossRef]
17. Borah, D.; Das, N.; Das, N.; Bhattacharjee, A.; Sarmah, P.; Ghosh, K.; Chandel, M.; Rout, J.; Pandey, P.; Ghosh, N.N. Alga-mediated Facile Green Synthesis of Silver Nanoparticles: Photophysical, Catalytic and Antibacterial Activity. *Appl. Organomet. Chem.* **2020**, *34*, e5597. [CrossRef]
18. Fatima, R.; Priya, M.; Indurthi, L.; Radhakrishnan, V.; Sudhakaran, R. Biosynthesis of Silver Nanoparticles Using Red Algae *Portieria hornemannii* and Its Antibacterial Activity against Fish Pathogens. *Microb. Pathog.* **2020**, *138*, 103780. [CrossRef]
19. Alsammarraie, F.K.; Wang, W.; Zhou, P.; Mustapha, A.; Lin, M. Green Synthesis of Silver Nanoparticles Using Turmeric Extracts and Investigation of Their Antibacterial Activities. *Colloids Surf. B Biointerfaces* **2018**, *171*, 398–405. [CrossRef]
20. Fazelian, N.; Movafeghi, A.; Yousefzadi, M.; Rahimzadeh, M.; Zarei, M. Impact of Silver Nanoparticles on the Growth, Fatty Acid Profile, and Antioxidative Response of *Nannochloropsis oculata*. *Acta Physiol. Plant.* **2020**, *42*, 126. [CrossRef]
21. Ghazaei, F.; Shariati, M. Effects of Titanium Nanoparticles on the Photosynthesis, Respiration, and Physiological Parameters in *Dunaliella salina* and *Dunaliella tertiolecta*. *Protoplasma* **2020**, *257*, 75–88. [CrossRef]
22. He, M.; Yan, Y.; Pei, F.; Wu, M.; Gebreluel, T.; Zou, S.; Wang, C. Improvement on Lipid Production by *Scenedesmus obliquus* Triggered by Low Dose Exposure to Nanoparticles. *Sci. Rep.* **2017**, *7*, 15526. [CrossRef]
23. Saied, E.; Eid, A.M.; Hassan, S.E.-D.; Salem, S.S.; Radwan, A.A.; Halawa, M.; Saleh, F.M.; Saad, H.A.; Saied, E.M.; Fouda, A. The Catalytic Activity of Biosynthesized Magnesium Oxide Nanoparticles (MgO-NPs) for Inhibiting the Growth of Pathogenic Microbes, Tanning Effluent Treatment, and Chromium Ion Removal. *Catalysts* **2021**, *11*, 821. [CrossRef]
24. Shanab, S.M.M.; Partila, A.M.; Ali, H.E.A.; Abdullah, M.A. Impact of Gamma-Irradiated Silver Nanoparticles Biosynthesized from Pseudomonas Aeruginosa on Growth, Lipid, and Carbohydrates of *Chlorella vulgaris* and *Dictyochloropsis splendida*. *J. Radiat. Res. Appl. Sci.* **2020**, *14*, 70–81. [CrossRef]
25. Razack, S.A.; Duraiarasan, S.; Mani, V. Biosynthesis of Silver Nanoparticle and Its Application in Cell Wall Disruption to Release Carbohydrate and Lipid from *C. vulgaris* for Biofuel Production. *Biotechnol. Rep.* **2016**, *11*, 70–76. [CrossRef] [PubMed]
26. Zhu, S.; Wang, Y.; Huang, W.; Xu, J.; Wang, Z.; Xu, J.; Yuan, Z. Enhanced Accumulation of Carbohydrate and Starch in *Chlorella zofingiensis* Induced by Nitrogen Starvation. *Appl. Biochem. Biotechnol.* **2014**, *174*, 2435–2445. [CrossRef] [PubMed]

27. Liu, J.; Qiu, Y.; He, L.; Luo, K.; Wang, Z. Effect of Iron and Phosphorus on the Microalgae Growth in Co-Culture. *Arch. Microbiol.* **2020**, *203*, 733–740. [CrossRef]
28. Romero, N.; Visentini, F.F.; Márquez, V.E.; Santiago, L.G.; Castro, G.R.; Gagneten, A.M. Physiological and Morphological Responses of Green Microalgae *Chlorella vulgaris* to Silver Nanoparticles. *Environ. Res.* **2020**, *189*, 109857. [CrossRef]
29. Deng, X.-Y.; Cheng, J.; Hu, X.-L.; Wang, L.; Li, D.; Gao, K. Biological Effects of TiO_2 and CeO_2 Nanoparticles on the Growth, Photosynthetic Activity, and Cellular Components of a Marine Diatom *Phaeodactylum tricornutum*. *Sci. Total Environ.* **2017**, *575*, 87–96. [CrossRef]
30. Marchello, A.E.; Barreto, D.M.; Lombardi, A.T. Effects of Titanium Dioxide Nanoparticles in Different Metabolic Pathways in the Freshwater Microalga *Chlorella Sorokiniana* (Trebouxiophyceae). *Water Air Soil Pollut.* **2018**, *229*, 48. [CrossRef]
31. Johari, S.A.; Sarkheil, M.; Tayemeh, M.B.; Veisi, S. Influence of Salinity on the Toxicity of Silver Nanoparticles (AgNPs) and Silver Nitrate ($AgNO_3$) in Halophilic Microalgae, *Dunaliella salina*. *Chemosphere* **2018**, *209*, 156–162. [CrossRef]
32. Peng, X.; Palma, S.; Fisher, N.S.; Wong, S.S. Effect of Morphology of ZnO Nanostructures on Their Toxicity to Marine Algae. *Aquat. Toxicol.* **2011**, *102*, 186–196. [CrossRef]
33. Da Costa, C.H.; Perreault, F.; Oukarroum, A.; Melegari, S.P.; Popovic, R.; Matias, W.G. Effect of Chromium Oxide (III) Nanoparticles on the Production of Reactive Oxygen Species and Photosystem II Activity in the Green Alga *Chlamydomonas reinhardtii*. *Sci. Total Environ.* **2016**, *565*, 951–960. [CrossRef]
34. Pirzadah, T.B.; Malik, B.; Salam, S.T.; Ahmad Dar, P.; Rashid, S. Impact of Heavy Metal Stress on Plants and the Role of Various Defense Elements. *Iran. J. Plant Physiol.* **2019**, *9*, 2883–2900.
35. Kaliamurthi, S.; Selvaraj, G.; Cakmak, Z.E.; Korkmaz, A.D.; Cakmak, T. The Relationship between *Chlorella* sp. and Zinc Oxide Nanoparticles: Changes in Biochemical, Oxygen Evolution, and Lipid Production Ability. *Process Biochem.* **2019**, *85*, 43–50. [CrossRef]
36. El-Naggar, N.E.-A.; Hussein, M.H.; Shaaban-Dessuuki, S.A.; Dalal, S.R. Production, Extraction and Characterization of *Chlorella vulgaris* Soluble Polysaccharides and Their Applications in AgNPs Biosynthesis and Biostimulation of Plant Growth. *Sci. Rep.* **2020**, *10*, 3011. [CrossRef] [PubMed]
37. Shariati, F.; Ayatallahzadeh Shirazi, M. Effect of SiO_2 Nanoparticles on Chlorophyll, Carotenoid and Growth of Green Micro-Algae *Dunaliella salina*. *Nanomed. Res. J.* **2019**, *4*, 164–175.
38. Sandhya, S.V.; Vijayan, K.K. Biogenesis of Silver Nanoparticles by Marine Bacteria *Labrenzia* sp. Mab 26 Associated with *Isochrysis galbana*. *Curr. Sci.* **2020**, *119*, 1830–1833. [CrossRef]
39. Al-Khazali, Z.K.M.; Alghanmi, H.A. Influence of Different Concentrations of Nano-Magnesium Oxide on the Growth of *Coelastrella terrestris*. *J. Phys. Conf. Ser.* **2019**, *1234*, 12070. [CrossRef]
40. Serif, M.; Dubois, G.; Finoux, A.-L.; Teste, M.-A.; Jallet, D.; Daboussi, F. One-Step Generation of Multiple Gene Knock-Outs in the Diatom *Phaeodactylum tricornutum* by DNA-Free Genome Editing. *Nat. Commun.* **2018**, *9*, 3924. [CrossRef]
41. Patil, P.D.; Gude, V.G.; Mannarswamy, A.; Deng, S.; Cooke, P.; Munson-McGee, S.; Rhodes, I.; Lammers, P.; Nirmalakhandan, N. Optimization of Direct Conversion of Wet Algae to Biodiesel under Supercritical Methanol Conditions. *Bioresour. Technol.* **2011**, *102*, 118–122. [CrossRef]
42. Hussain, J.; Wang, X.; Sousa, L.; Ali, R.; Rittmann, B.E.; Liao, W. Using Non-Metric Multi-Dimensional Scaling Analysis and Multi-Objective Optimization to Evaluate Green Algae for Production of Proteins, Carbohydrates, Lipids, and Simultaneously Fix Carbon Dioxide. *Biomass Bioenergy* **2020**, *141*, 105711. [CrossRef]
43. Yin, Z.; Zhu, L.; Li, S.; Hu, T.; Chu, R.; Mo, F.; Hu, D.; Liu, C.; Li, B. A Comprehensive Review on Cultivation and Harvesting of Microalgae for Biodiesel Production: Environmental Pollution Control and Future Directions. *Bioresour. Technol.* **2020**, *301*, 122804. [CrossRef]
44. Hauser-Davis, R.A.; Lavradas, R.T.; Monteiro, F.; Rocha, R.C.C.; Bastos, F.F.; Araújo, G.F.; Júnior, S.F.S.; Bordon, I.C.; Correia, F.V.; Saggioro, E.M. Biochemical Metal Accumulation Effects and Metalloprotein Metal Detoxification in Environmentally Exposed Tropical Perna Perna Mussels. *Ecotoxicol. Environ. Saf.* **2021**, *208*, 111589. [CrossRef]
45. Ren, H.-Y.; Dai, Y.-Q.; Kong, F.; Xing, D.; Zhao, L.; Ren, N.-Q.; Ma, J.; Liu, B.-F. Enhanced Microalgal Growth and Lipid Accumulation by Addition of Different Nanoparticles under Xenon Lamp Illumination. *Bioresour. Technol.* **2020**, *297*, 122409. [CrossRef] [PubMed]
46. Kadar, E.; Rooks, P.; Lakey, C.; White, D.A. The Effect of Engineered Iron Nanoparticles on Growth and Metabolic Status of Marine Microalgae Cultures. *Sci. Total Environ.* **2012**, *439*, 8–17. [CrossRef]
47. Rocha, A.A.; Wilde, C.; Hu, Z.; Nepotchatykh, O.; Nazarenko, Y.; Ariya, P.A. Development of a Hybrid Photo-Bioreactor and Nanoparticle Adsorbent System for the Removal of CO_2, and Selected Organic and Metal Co-Pollutants. *J. Environ. Sci.* **2017**, *57*, 41–53. [CrossRef] [PubMed]
48. Katare, A.K.; Singh, B.; Shukla, P.; Gupta, S.; Singh, B.; Yalamanchili, K.; Kulshrestha, N.; Bhanwaria, R.; Sharma, A.K.; Sharma, S. Rapid Determination and Optimisation of Berberine from Himalayan *Berberis lycium* by Soxhlet Apparatus Using CCD-RSM and Its Quality Control as a Potential Candidate for COVID-19. *Nat. Prod. Res.* **2020**, *36*, 868–873. [CrossRef]
49. Aydın, M.; Uslu, S.; Çelik, M.B. Performance and Emission Prediction of a Compression Ignition Engine Fueled with Biodiesel-Diesel Blends: A Combined Application of ANN and RSM Based Optimization. *Fuel* **2020**, *269*, 117472. [CrossRef]

50. Elshobary, M.E.; Zabed, H.M.; Qi, X.; El-Shenody, R.A. Enhancing Biomass and Lipid Productivity of a Green Microalga *Parachlorella kessleri* for Biodiesel Production Using Rapid Mutation of Atmospheric and Room Temperature Plasma. *Biotechnol. Biofuels Bioprod.* **2022**, *15*, 122. [CrossRef] [PubMed]
51. Huo, S.; Basheer, S.; Liu, F.; Elshobary, M.; Zhang, C.; Qian, J.; Xu, L.; Arslan, M.; Cui, F.; Zan, X. Bacterial Intervention on the Growth, Nutrient Removal and Lipid Production of *Filamentous oleaginous* Microalgae *Tribonema* sp. *Algal Res.* **2020**, *52*, 102088. [CrossRef]
52. Elshobary, M.E.; Abo-Shady, A.M.; Khairy, H.M.; Essa, D.; Zabed, H.M.; Qi, X.; Abomohra, A.E.-F. Influence of Nutrient Supplementation and Starvation Conditions on the Biomass and Lipid Productivities of *Micractinium reisseri* Grown in Wastewater for Biodiesel Production. *J. Environ. Manag.* **2019**, *250*, 109529. [CrossRef]
53. Zhang, L.; Cheng, J.; Pei, H.; Pan, J.; Jiang, L.; Hou, Q.; Han, F. Cultivation of Microalgae Using Anaerobically Digested Effluent from Kitchen Waste as a Nutrient Source for Biodiesel Production. *Renew. Energy* **2018**, *115*, 276–287. [CrossRef]
54. El Shafay, S.M.; Gaber, A.; Alsanie, W.F.; Elshobary, M.E. Influence of Nutrient Manipulation on Growth and Biochemical Constituent in *Anabaena variabilis* and *Nostoc muscorum* to Enhance Biodiesel Production. *Sustainability* **2021**, *13*, 9081. [CrossRef]